EPA/600/2-91/014
April 1991

DENITRIFICATION IN NONHOMOGENEOUS LABORATORY SCALE AQUIFERS: 4. HYDRAULICS, NITROGEN CHEMISTRY, AND MICROBIOLOGY IN A SINGLE LAYER

by

F. T. Lindstrom, L. Boersma, D. Myrold, and M. Barlaz

Department of Soil Science
Oregon State University
Corvallis, OR 97331

Cooperative Agreement CR 814502-01-1

Project Officer

Thomas E. Short
Processes and System Research Division
Robert S. Kerr Environmental Research Laboratory
Ada, OK 74820

ROBERT S. KERR ENVIRONMENTAL RESEARCH LABORATORY
OFFICE OF RESEARCH AND DEVELOPMENT
U.S. ENVIRONMENTAL PROTECTION AGENCY
ADA, OK 74820

DISCLAIMER

The information in this document has been funded wholly or in part by the United States Environmental Protection Agency under Assistance Agreement No. CR-814502-01-1 to Oregon State University. It has been subjected to the Agency's peer and administrative review, and it has been approved for publication as an EPA document. Mention of trade names or commercial products does not constitute endorsement or recommendation for use.

FOREWORD

EPA is charged by congress to protect the Nation's land, air and water systems. Under a mandate of national environmental laws focused on air and water quality, solid waste management and control of toxic substances, pesticides, noise, and radiation, the agency strives to formulate and implement actions which lead to a compatible balance between human activities and the ability of natural systems to support and nurture life.

The Robert S. Kerr Environmental Research Laboratory is the agency's center of expertise for investigation of the soil and subsurface environment. Personnel at the laboratory are responsible for management of research programs to: (a) determine the fate, transport and transformation rates of pollutants in the soil, the unsaturated zone and the saturated zones of the subsurface environment; (b) define the processes to be used in characterizing the soil and subsurface environment as a receptor of pollutants; (c) develop techniques for predicting the effects of pollutants on groundwater, soil and indigenous organisms; and (d) define and demonstrate the applicability and limitations of using natural processes, indigenous to the soil and subsurface environment, for the protection of this resource.

Laboratory scale, physical, test aquifers are increasingly being used for the study of transport and fate processes. It is generally less expensive to evaluate hypotheses for pollution fate and transport using laboratory scale aquifers than to work under field conditions. Furthermore, numerical models of the fate and transport of chemicals in aquifers are now rapidly coming within the reach of environmental scientists. These models are even cheaper and faster to operate than are laboratory systems. The current investigation will analyze the ability of laboratory aquifers to validate mathematical models. This report presents a mathematical analysis of two dimensional horizontal transport and fate processes in aquifers. This analysis led to development of a computerized model. In further development (later report), results obtained from the mathematical model will be compared to the results obtained in a laboratory test aquifer used to study in situ denitrification as the first test case.

Clinton W. Hall

Clinton W. Hall
Director
Robert S. Kerr Environmental
Research Laboratory

ABSTRACT

A two dimensional mathematical model for simulating the transport and fate of organic chemicals in a laboratory scale, single layer aquifer is presented. The aquifer can be nonhomogeneous and anisotropic with respect to fluid flow properties. The physical model for which this mathematical model has been developed is assumed to have open inlet and outlet ends and to be bounded by impermeable walls on all sides. The mathematical model allows placement of fully penetrating injection and/or extraction wells anywhere in the flow field. The inlet and outlet boundaries have user prescribed hydraulic pressure fields. The steady state hydraulic pressure field is obtained first, by using the two-dimensional Darcy flow law and the continuity equation.

Separate dynamic transport and fate equations are then set up for each of four dissolved chemicals, which include a substrate, nutrients, oxygen, and nitrate. Two equations, modeling the local growth and decay of two microbial populations, one operating with either oxygen or nitrogen, the other only with oxygen, are coupled to the transport and fate equations. The four chemical transport and fate equations are then solved in terms of user prescribed initial conditions. Boundary conditions are zero flow at the top, bottom, and sidewalls and accounting of mass at the inlet and exit ports. The model accounts for the major physical processes of dispersion and advection, and also can account for linear equilibrium sorption, four first order loss processes, including irreversible chemical reaction and/or dissolution into the organic phase, and irreversible binding in the sorbed state. The loss of substrate, nitrate, nutrient, and oxygen is accounted for by modified Monod kinetic type rate rules. The chemical may be released internally by distributed sources that do not perturb the flow field, or from fully penetrating injection wells. Chemical compound may also enter at the inlet boundary. Chemical mass balance type inlet and outlet boundary conditions are used. The solution to the field equation for hydraulic pressure is approximated by the space centered finite difference method using the strongly implicit procedure (SIP) with a user specified heuristic for choosing the iteration parameter. A solution to the transport and fate equations is approximated with a forward in time Euler-Lagrange time integrator applied to the chemical transport and fate semi-discretization. A user manual for the model is available in a separate document.

CONTENTS

Disclaimer..... ii

Foreword..... iii

Abstract..... iv

List of Figures..... vii

1. Introduction..... 1

2. Statement of the Problem..... 3

   1. Introduction..... 3

   2. Physical Aquifers at RSKERL..... 3

   3. Long-term Goals of the Mathematical Modeling Effort 4

   4. Assumptions Underlying Model LT3VSI..... 5

3. Nomenclature and Notation used for the Model..... 8

   1. Fluid Flow Field..... 8

   2. Chemical Transport and Fate Field..... 9

   3. Chemical Transformations..... 11

4. Fluid Flow Field..... 15

   1. Statement of the Problem..... 15

   2. Approximation of the Fluid Flow Equations..... 17

   3. Boundary Conditions..... 21

   4. Solution of the Linear System of Equations..... 22

   5. Velocity Components..... 23

CONTENTS (continued)

5. Chemical Transport and Fate Model..... 26

1. Transport and Fate Equations..... 26

2. Initial Data, Boundary Data, and Total Chemical Mass 35

3. Approximate Solution for the Transport and Fate Equations..... 40

4. Boundary Conditions for Approximate Concentration Field..... 45

5. Approximate Microbial Populations..... 51

6. Stability Considerations..... 53

6. Conclusions for the Model..... 55

7. Literature Cited..... 57

Appendix A..... 61

FIGURES

Figure 1.	Schematic diagram of physical models used for the studies of aquifer restoration at Robert S. Kerr Environmental Research Laboratory	4
Figure 2.	Schematic diagram of the physical model used for studies of transport and fate problems	7
Figure 3.	Local interior region of lattice points showing subregion D_{ij}	18
Figure 4.	Schematic diagram of the physical aquifer used for testing the mathematical model, showing mixing chambers at inlet and outlet ends	37
Figure 5.	Details of the use of the "Gaussian pill box" concept in the mixing chambers, showing flow orientation, and positions where mathematical terms were defined	37
Figure 6.	Relations of the various subregions of the overall space-time cylinder and the superimposed set of lattice points	41

DENITRIFICATION IN NONHOMOGENEOUS LABORATORY SCALE AQUIFERS: 4. HYDRAULICS, NITROGEN CHEMISTRY, AND MICROBIOLOGY IN A SINGLE LAYER

1. INTRODUCTION

This is the fourth report in a series describing mathematical models for denitrification processes in nonhomogeneous, laboratory scale aquifers. This report expands the mathematical model developed in Volume 1 (Lindstrom and Boersma, 1990) of the series. The nitrogen chemistry and microbiological processes that occur in a single layer, saturated, aquifer have been added to this model. This development is an intermediate step towards completing a fully three dimensional model that applies to an aquifer made up of three layers. Such an aquifer is used at the USEPA Laboratory at Ada, Oklahoma for testing bioremediation processes for denitrification. Details of the bioremediation processes being investigated and the justification for this research were described in detail in Volume 1 of this series (Lindstrom and Boersma, 1990).

The success of biological denitrification methods depends on availability of a fundamental understanding of the transport and fate processes. In addition, knowledge about the important limiting factors, or limiting system properties must be acquired. Therefore, the immediate objective was to develop a preliminary mathematical model (Lindstrom and Boersma, 1990) and associated computer code (Bachelor et al., 1990) to describe substrate injection into a single layer, laboratory scale aquifer and to use the model in a sensitivity manner to assess the magnitude of the physical and biological factors controlling aquifer denitrification processes and identify those which can be manipulated to

enhance the process (Boersma and Lindstrom, 1990). The sensitivity analysis is reported in the associated documents Volume 2 (Bachelor et al., 1990) and Volume 3, which describes applications to 2-D non-homogeneous flow fields (Boersma and Lindstrom, 1990).

The preliminary mathematical model addresses aquifer fluid transport phenomena including perturbations due to the presence of injection and withdrawal wells. Solute movement includes advection, dispersion, molecular diffusion, and simple first order chemical and/or biological reactions in the aquifer. The mathematical modeling effort presented here is part of an ongoing study of aquifer restoration being conducted by the U.S. Environmental Protection Agency at the R. S. Kerr Environmental Research Laboratory in Ada, Oklahoma. One of the long-term goals of this study is development of a mathematical model of aquifer denitrification processes enhanced by stimulation of microbial populations. The experience gained from developing the preliminary model was used to develop the two-dimensional model for the simultaneous transport and fate of nitrate, and oxygen, substrate, e.g. methanol and inorganic nutrients, in the single layer aquifer, described in this report. Two independently operating microbial populations are included in the model, both using modified Monod kinetics. The model, called LT3VSI, is described in this document.

2. STATEMENT OF THE PROBLEM

2.1 Introduction

Laboratory scale, physical models of aquifers are increasingly being used for the study of aquifer processes. Often it is less expensive to evaluate hypotheses for restoration procedures using laboratory scale models than to work under field conditions. Aquifer restoration methods are not without hazards. Biorestoration processes may alter the hydraulic properties of the aquifer.

Furthermore, numerical models of the transport and fate of chemicals in aquifers are now rapidly coming within the reach of environmental scientists. These models, once validated for the systems they are designed to simulate, are often cheaper and much faster to operate in real time response than the physical models. Thus the combination of mathematical models and laboratory scale models presents a cost effective and time efficient method for the study of bioremediation of contaminated aquifers.

2.2 Physical Aquifers at RSKERL

Two large (4 ft wide, 4 ft high, 16 ft long) physical aquifers (Figure 1) were constructed at the USEPA Robert S. Kerr Environmental Research Laboratory in Ada, Oklahoma. Each aquifer contains three horizontal layers of material, with each layer assumed to be homogeneous and isotropic with respect to water flow. These systems can be used for validation of mathematical models that simulate the hydrodynamic pressure distribution (Yates, 1988a,b), for the study of transport and fate of chemicals, and for evaluation of the growth characteristics of

indigenous microbial populations. The physical aquifers are also used for the study of proposed physical and biological remediation schemes.

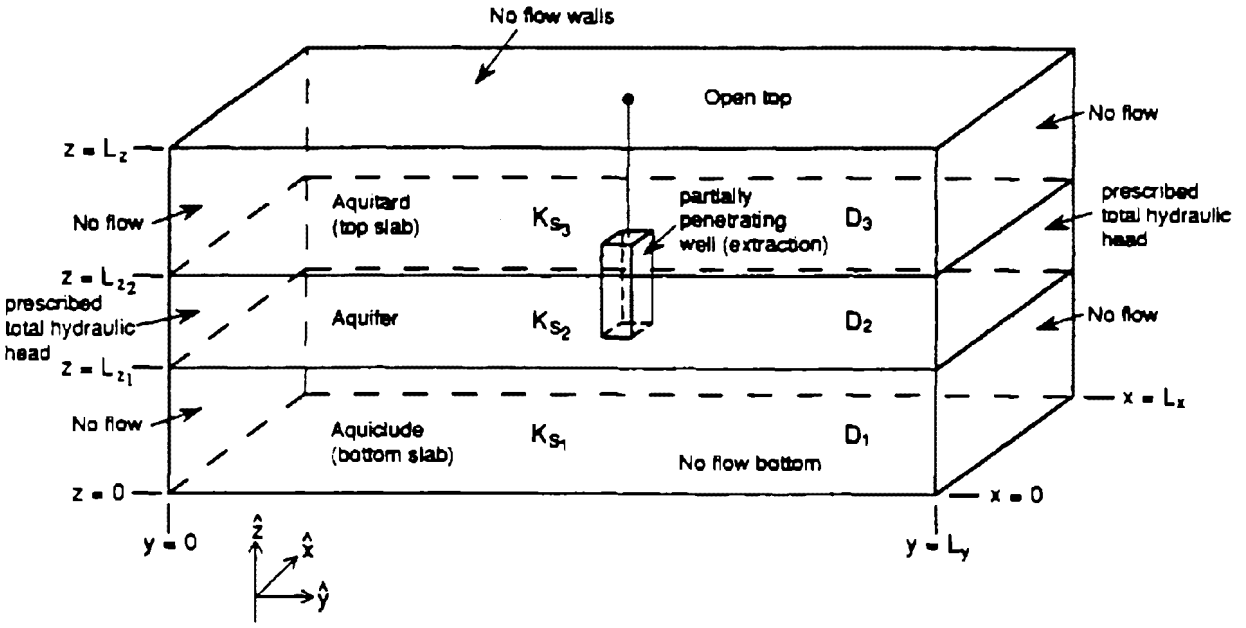

Figure 1. Schematic diagram of physical models used for the studies of aquifer restoration at Robert S. Kerr Environmental Research Laboratory

2.3 Long-term Goals of the Mathematical Modeling Effort

The goal of the present mathematical modeling effort is to describe the fate and transport of contaminants in the physical models. This work includes two-dimensional mathematical modeling of the steady state hydraulics and simultaneous transport and fate of the dissolved oxygen, nutrients (such as phosphorus), a carbon based substrate (for example methanol), and dissolved nitrate. Also included are two microbial populations which change in space and time. The mathematical model will be used to study scenarios for biorestoration of aquifers contaminated with nitrates.

The procedures being followed to achieve these goals include several steps. The first step was development of a preliminary model of the transport and fate of chemical compounds, with constant first-order loss processes and linear equilibrium sorption assumptions. This model is for two space dimensions and simulates only the "aquifer" slab of the physical model. The second step was to use the preliminary, two-dimensional model, called LT2VSI, for preliminary numerical studies of several scenarios for injection and/or extraction well placement. The third step was to expand LT2VSI by including four chemical compounds and two microbial populations. This model, referred to as LT3VSI, is the subject of this report.

2.4 Assumptions Underlying Model LT3VSI

The RSKERL physical models have been constructed in such a way that homogeneous and isotropic soil slabs were obtained. They have impermeable (no flow) side walls, an open top, partially open ends, and an impermeable lower or bottom boundary. The assumptions regarding the walls and the bottom made in the preliminary mathematical model LT2VSI (Figure 2) reflect these conditions with the exception that the top boundary was assumed to be a "no flow" boundary. The hydraulic head distributions at the completely open inlet and exit boundaries are prescribed in model LT2VSI and fully penetrating injection and extraction wells may be present. Model LT2VSI was developed for a single-layer of soil representing the aquifer part of the three soil layers making up the RSKERL aquifers.

This report describes an extension of the preliminary model which is referred to as LT3VSI. The hydraulics in LT3VSI are the same as in LT2VSI. The important features of LT3VSI are:

1) Two-dimensional, horizontal, steady state, fluid flow field defined by a hydraulic head field which depends on appropriate Dirichlet and Neumann boundary conditions and characterizing the spatial dependency of the longitudinal and transverse components of the hydraulic conductivity tensor at saturation.

2) Simultaneous two-dimensional transport and fate of four dissolved chemicals, i.e.: oxygen, substrate, nutrient, and nitrate in the nonhomogeneous aquifer. The distribution of chemicals is affected by

   i) advection and dispersion in both the longitudinal and transverse directions,

   ii) linear equilibrium adsorption/desorption processes on each of the porous medium fractions,

   iii) three different first-order loss processes

      a) chemical reaction with other soil components in the free phase,

      b) other irreversible processes in the free phase,

      c) chemical reaction in the sorbed phase,

   iv) modified Monod microbial degradation kinetics of the substrate system including oxygen, nutrients, and nitrate in addition to two microbial populations,

   v) the presence of zero order sources of the chemicals,

vi) appropriate Dirichlet and no flux Neumann boundary conditions with a provision for nonzero initial distribution of the chemicals,

vii) presence of fully penetrating injection and/or extraction wells.

It is assumed that most, if not all, of the chemical and biological process coefficients are at least once continuously differentiable functions of the transverse coordinate x and the longitudinal coordinate y (Figure 2).

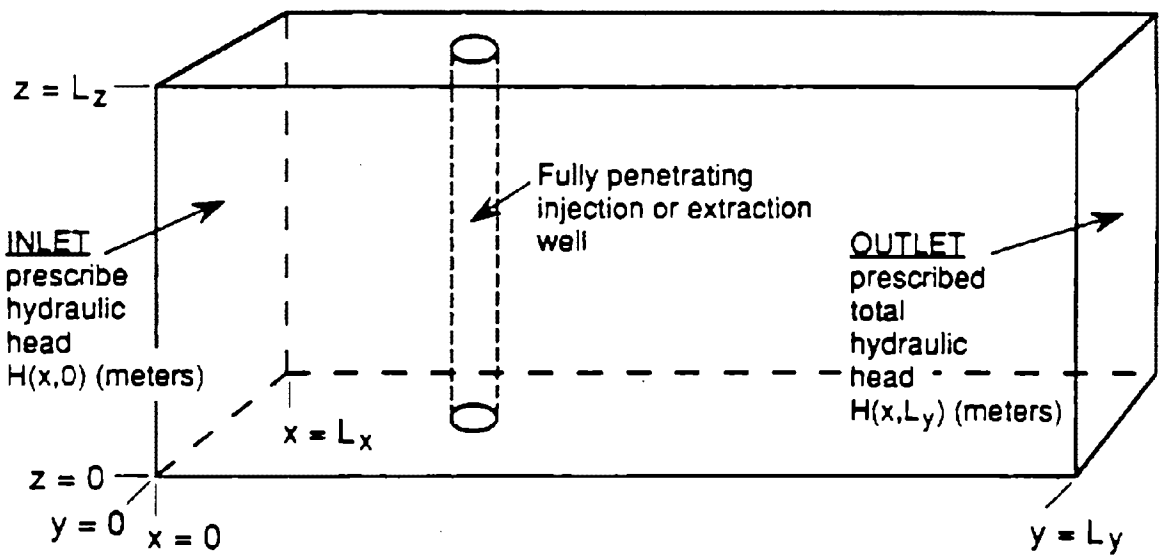

Figure 2. Schematic diagram of the physical model used for studies of transport and fate problems

3. NOMENCLATURE AND NOTATION USED FOR THE MODEL

3.1. Fluid Flow Field

A	A real nonsymmetric positive definite $(N_x-1) \bullet (N_y-1)$ by $(N_x-1) \bullet (N_y-1)$ array used for computing $\underset{\sim}{\tilde{H}}$	$m^{-1}\ day^{-1}$
$\underset{\sim}{b}$	vector of boundary data in the hydraulic head field	day^{-1}
D	$\{x,y)$ in $R^2 \mid (0 < x < L_x) \times (0 < y < L_y)\}$	dimensionless
H	hydraulic head field	m water
$\underset{\sim}{H}$	vector of approximate hydraulic heads	m water
$\tilde{H}_{ij}$	approximate hydraulic head field at location (x_i, y_j)	m water
H_{in}	hydraulic head field at $y = 0$	m water
H_{out}	hydraulic head field at $y = L_y$	m water
K_{sxx}	transverse component of saturated hydraulic conductivity tensor	$m\ day^{-1}$
K_{syy}	longitudinal component of saturated hydraulic conductivity tensor	$m\ day^{-1}$
L_x	transverse dimension (width) of aquifer	m
L_y	longitudinal dimension (length) of aquifer	m
L_w	vertical dimension of aquifer	m
N_x	number of subintervals in interval $[0, L_x]$. There are N_x-1 internal nodes on the transverse coordinate and N_x+1 total nodes along this same coordinate.	
N_y	number of subintervals in interval $[0, L_y]$. There are N_y-1 internal nodes on the longitudinal coordinate and N_y+1 total nodes along this same coordinate.	
$\underset{\sim}{q}$	Darcy velocity vector	$m\ day^{-1}$
q_x	x-component of Darcy velocity vector	$m\ day^{-1}$
q_y	y-component of Darcy velocity vector	$m\ day^{-1}$

Q	mass density rate function for sources and/or sinks; these rules must be small relative to the inlet flow rates	kg m^{-3} day^{-1}
Q_{inj}	mass density rate of injection well	kg m^{-3} day^{-1}
Q_{out}	mass density rate of extraction well	kg m^{-3} day^{-1}
$\underset{\sim}{U}$	average seepage velocity vector	m day^{-1}
U_x	x-component of average seepage velocity vector	m day^{-1}
U_y	y-component of average seepage velocity vector	m day^{-1}
V_{REV}	representative elementary volume	m^3
x	transverse spatial component	m
y	longitudinal spatial component	m
α_{ij}	ijth correction factor used for correcting the area estimate for adjacent injection and/or pumping wells	
ϵ	volume porosity of porous medium	m^3 m^{-3}
ρ_w	density of water	kg m^{-3}
∇	"del" or nabla vector operator	m^{-1}
∇^2	Laplace operator	m^{-2}

3.2. Chemical Transport and Fate Field

The superscript symbol * in the equations denotes one of the four chemicals of interest in the transport and fate fields, as follows: Nu for nutrient; S for substrate; O for oxygen; and Ni for nitrate.

C^*	distribution of chemical concentration in the free phase	kg m^{-3}
C^*_{in}	chemical concentration in the inlet end mixing tank	kg m^{-3}
C^*_{out}	chemical concentration in the outlet end mixing tank	kg m^{-3}
C^*_{sour}	chemical concentration of the injection wells	kg^{-1}

C_o^*	chemical concentration in feed stream	kg m^{-3}
D_{cin}^*	average dispersion coefficient in the inlet tank	m^2 day^{-1}
D_{cout}^*	average dispersion coefficient in the outlet tank	m^2 day^{-1}
$D_{L_0}^*$	molecular diffusion coefficient of compound in free solution	m^2 day^{-1}
D_{xx}^*	x-component of dispersion	m^2 day^{-1}
D_{yy}^*	y-component of dispersion	m^2 day^{-1}
D_{xy}^*	cross component of dispersion	m^2 day^{-1}
L_{in}	length of the inlet end mixing tank	m
L_{out}	length of the outlet end mixing tank	m
L_{yin}	distance from the plane y=0 to the center of the inlet end mixing tank	m
L_{yout}	distance from the plane $y=L_y$ to the center of the outlet end mixing tank	m
$M_{in}^*(t)$	mass of compound * in the inlet tank at time t days	kg
$M_{out}^*(t)$	mass of compound * in the outlet tank at time t days	kg
Q_{so}^*	source rate density from buried sources	kg m^{-3} day^{-1}
R^*	retention parameter	dimensionless
t	elapsed time in days from commencing injection and/or pumping	days
$\|U_x\|$	magnitude of x-component of the seepage velocity	m day^{-1}
$\|U_y\|$	magnitude of y-component of the seepage velocity	m day^{-1}
V_{in}	average flow velocity in inlet tank	m day^{-1}
V_{out}	average flow velocity in outlet tank	m day^{-1}
α_{dispx}	x-component of dispersivity	m
α_{dispy}	y-component of dispersivity	m

α_{tort}	tortuosity factor	dimensionless
Δt	time increment $t_{n+1} = t_n + \Delta t$	days

3.3 Chemical Transformations

K^*_{org}	linear equilibrium distribution constant for organics expressed in volume per unit mass of organic matter	$m^3\ kg^{-1}_{org}$
K^*_{ws}	linear equilibrium distribution constant for mildly sorbing surfaces, expressed as volume per unit mass of mildly sorbing particles	$m^3\ kg^{-1}_{ws}$
K^*_s	linear equilibrium distribution constant for strongly sorbing surfaces, expressed as volume per unit mass of strongly sorbing particles	$m^3\ kg^{-1}_s$
K^1_{so}	one half maximum saturation constant for population 1 utilizing the substrate	$kg\ m^{-3}$
K^1_o	one half maximum saturation constant for population 1 utilizing oxygen	$kg\ m^{-3}$
K^1_{onu}	one half maximum saturation constant for population 1 utilizing nutrients	$kg\ m^{-3}$
K^2_{so}	one half maximum saturation constant for population 2 utilizing the substrate	$kg\ m^{-3}$
K^2_o	one half maximum saturation constant for population 2 utilizing oxygen	$kg\ m^{-3}$
K^2_{onu}	one half maximum saturation constant for population 2 utilizing nutrients	$kg\ m^{-3}$
K^1_{sni}	one half maximum nitrate based saturation constant for population 1 utilizing substrate	$kg\ m^{-3}$
K^1_{ni}	one half maximum nitrate based saturation constant for population 1 utilizing nitrate	$kg\ m^{-3}$
K^1_{ninu}	one half maximum nitrate based saturation constant for population 1 utilizing nutrients	$kg\ m^{-3}$
K^1_{oni}	one half maximum nitrate based inhibition constant for population 1 utilizing nitrate instead of oxygen as its electron acceptor	$kg\ m^{-3}$

K^1_{som}	one half saturation coefficient for maintenance in population 1	kg m^{-3}
K^2_{som}	one half saturation coefficient for maintenance in population 2	kg m^{-3}
$N_1(t)$	population 1 cell mass in the unit pore volume at elapse time t days in microbial mass per unit soil mass	kg kg^{-1}
$N_2(t)$	population 2 cell mass in the unit pore volume at elapse time t days in microbial mass per unit soil mass	kg kg^{-1}
r^1_{sonu}	oxygen utilization rate by microbial population 1 in substrate mass per unit cell mass per day	kg kg^{-1} day^{-1}
r^1_{sninu}	nitrate utilization rate by microbial population 1 in substrate mass per unit cell mass per day	kg kg^{-1} day^{-1}
r^2_{sonu}	oxygen utilization rate by microbial population 2 in substrate mass per unit cell mass per day	kg kg^{-1} day^{-1}
S	chemical concentration distribution in the sorbed phase for linear equilibrium	kg m^{-3}
Y^1_{so}	yield coefficient for microbial population 1 utilizing oxygen in cell mass per unit mass of substrate	kg kg^{-1}
Y^2_{so}	yield coefficient for microbial population 2 utilizing oxygen in cell mass per unit mass of substrate	kg kg^{-1}
Y^1_{sni}	yield coefficient for microbial population 1 utilizing nitrate in cell mass per unit mass of substrate	kg kg^{-1}
M_o/M_t	mass fraction of organic matter in porous medium	kg kg^{-1}
M_{ws}/M_t	mass fraction of weakly sorbing particles in porous medium	kg kg^{-1}
M_s/M_t	mass fraction of strongly sorbing particles in porous medium	kg kg^{-1}

α_o^1	oxygen maintenance rate coefficient based on population 1 using oxygen under aerobic conditions in mass of oxygen per unit mass of cells	$kg\ kg^{-1}$
α_o^2	oxygen maintenance rate coefficient based on population 2 using oxygen under aerobic conditions in mass of oxygen per unit mass of cells	$kg\ kg^{-1}$
α_{ni}^1	nitrate maintenance rate coefficient based on population 1 using nitrate under aerobic conditions in mass of nitrate per unit mass of cells	$kg\ kg^{-1}$
δ^1	constant for death rate of population 1	day^{-1}
δ^2	constant for death rate of population 2	day^{-1}
η_{ni}^1	coefficient for nitrate use based on population 1 and anaerobic conditions	$kg\ kg^{-1}$
γ_o^1	coefficient for oxygen use based on population 1 using oxygen under aerobic conditions in mass of oxygen per unit mass of substrate	$kg\ kg^{-1}$
γ_o^2	coefficient for oxygen use based on population 2 using oxygen under aerobic conditions in mass of oxygen per unit mass of substrate	$kg\ kg^{-1}$
λ^*	first-order free phase loss rate constant for irreversible loss processes, e.g. chemical reactions	day^{-1}
λ_{irr}^{s*}	first-order sorbed phase loss rate constant for irreversible processes	day^{-1}
Λ^*	overall first-order loss processes rate coefficient	day^{-1}
$\lambda^*(x,y,t)$	loss rate function of compound * due to microbial processes	$kg^*\ m^{-3}\ day^{-1}$
ψ_o^1	nutrient use coefficient based on population 1 and oxygen conditions in nutrient mass per unit mass of substrate	$kg^*\ m^{-3}\ day^{-1}$
ψ_o^2	nutrient use coefficient based on population 2 and oxygen conditions in mass of nutrient per unit mass of substrate	$kg^*\ m^{-3}\ day^{-1}$

ρ_b	average bulk density of porous medium	kg m^{-3}
ρ_{ws}	average particle density of weakly sorbing fraction	kg m^{-3}
ρ_s	average particle density of strongly sorbing fraction	kg m^{-3}
ρ_{org}	average particle density of organic matter fraction	kg m^{-3}
θ^1_{ni}	nutrient use coefficient based on population 1 using nitrate under anaerobic conditions in nutrient mass per unit mass of substrate	kg m^{-3}
μ^1_o	maximum specific growth rate for heterotrophic population 1	day^{-1}
μ^2_o	maximum specific growth rate for heterotrophic population 2	day^{-1}
μ^1_{ni}	maximum specific nitrate based on growth rate for heterotrophic population 1	day^{-1}

4. FLUID FLOW FIELD

4.1. Statement of the Problem

Figure 2 shows a schematic diagram of the single layer aquifer of the physical model, with water flowing into and out from the soil via open ends. Water can also be extracted or injected through fully penetrating injection and/or extraction wells. The transverse coordinate is x (m) and the longitudinal coordinate is y (m). The third coordinate L_w (m) represents aquifer thickness. The porous medium may be nonhomogeneous and anisotropic with respect to fluid flow properties and has impervious walls on all sides. These conditions allow evaluation of two-dimensional transport and fate.

The assumptions concerning the fluid flow field are:

1) The fluid flow field operates at steady state conditions at all times.

2) Any fluid flow perturbations introduced at the flow boundaries propagate extremely rapidly throughout the flow field, so that a new steady state is achieved instantly. Under these conditions the fluid storativity term in the fluid flow model may be neglected as shown for aquifers of the size considered here (Bodvarsson, 1984).

3) The aquifer material can be nonhomogeneous as well as anisotropic, with the principal components K_{sxx} and K_{syy} of the saturated hydraulic conductivity tensor assumed to be once continuously differentiable over the interior of the flow domain.

4) Dirichlet boundary conditions hold at both the inlet and outlet ends. H_{in} (m) at the inlet end and H_{out} (m) at the

outlet end are specified and assumed to extend across, $0 < x < L_x$.

5) No-flow Neumann or flux type boundary conditions are specified along the walls, i.e. the $x = 0$ and $x = L_x$ planes.

6) The Darcy velocity field components of the flow vector q(m day^{-1}) are defined by

$$\underset{\sim}{q} = (\epsilon\ U_x,\ \epsilon\ U_y) = (-K_{sxx}\ \frac{\partial H}{\partial x},\ -K_{syy}\ \frac{\partial H}{\partial y}) \ , \tag{4.1.1}$$

where K_{sxx} and K_{syy} are the transverse and longitudinal components (m day^{-1}) of the saturated hydraulic conductivity in the aquifer, ϵ is porosity, and H is the hydraulic head (m). The coordinate system has been chosen to coincide with the two principal directions of flow (Bear and Verruijt, 1987).

Combining equation (4.1.1) with the continuity equation for steady state conditions in a representative elementary volume (REV) in the aquifer, obtains

$$\nabla \bullet (\rho_w\ \epsilon\ \underset{\sim}{U}) = (Q_{inj} - Q_{out}) \ , \tag{4.1.2}$$

where ρ_w is the density of water (kg m^{-3}) is assumed constant, Q_{inj} is the fluid mass injection rate (kg m^{-3} day^{-1}) and Q_{out} is the fluid mass extraction rate (kg m^{-3} day^{-1}).

Substitution for (ϵ U) in equation (4.1.2) leads to the well known Poisson problem in potential field theory:

$$\rho_w \left[\frac{\partial(-K_{sxx}\ \frac{\partial H}{\partial x})}{\partial x} + \frac{\partial(-K_{syy}\ \frac{\partial H}{\partial y})}{\partial y}\right] = \rho_w \left[\frac{\partial(\epsilon\ U_x)}{\partial x} + \frac{\partial(\epsilon\ U_y)}{\partial y}\right]$$

$$= + (Q_{inj} - Q_{out}), \tag{4.1.3}$$

where ϵ, K_{sxx}, and K_{syy} are assumed to be once continuously differentiable functions of x and y inside the flow domain.

Boundary conditions to be satisfied at all times, are written according to assumptions 4 and 5 as follows:

i) along $y = 0$ (inlet end): $H(x,0) = H_{in}(x)$, $0 \le x \le L_x$, (4.1.4)

ii) along $y = L_y$ (outlet end): $H(x,L_y) = H_{out}(x)$, $0 \le x \le L_x$, (4.1.5)

iii) along $x = 0$: $\frac{\partial H}{\partial x} = 0$, (4.1.6)

iv) along $x = L_x$: $\frac{\partial H}{\partial x} = 0$. (4.1.7)

Since K_{sxx} and K_{syy} are usually not constant and may vary by several orders of magnitude over the interior of the flow domain, analytic solutions of equation (4.1.3), subject to boundary conditions (4.1.4) through (4.1.7), are not obtainable. For isotropic and homogeneous porous media, Lindstrom et al. (1989) give an analytical representation in terms of a double sum infinite series of trigonometric functions, i.e. an eigenfunction solution procedure. However, even in the very special isotropic case of $K_{sxx} = K_{syy} = K_s$, where K_s is a constant, the solutions are usually very slow to converge. Thousands if not millions of terms are necessary to achieve the required number of significant digits in each velocity component. Thus, the hydraulic head field on $\mathcal{D}$, the interior of the flow domain, is usually approximated by means of finite difference or finite element methods.

4.2. Approximation of the Fluid Flow Equations

Figure 3 shows a local region of $\mathcal{D}$ on which a lattice of nodal points has been superimposed. $\mathcal{D}$ is the set of all (x,y)'s in R^2 such

that $\{[0 < x < L_x] \times [0 < y < L_y]\}$, with nonhomogeneous nodal spacing allowed in both coordinates.

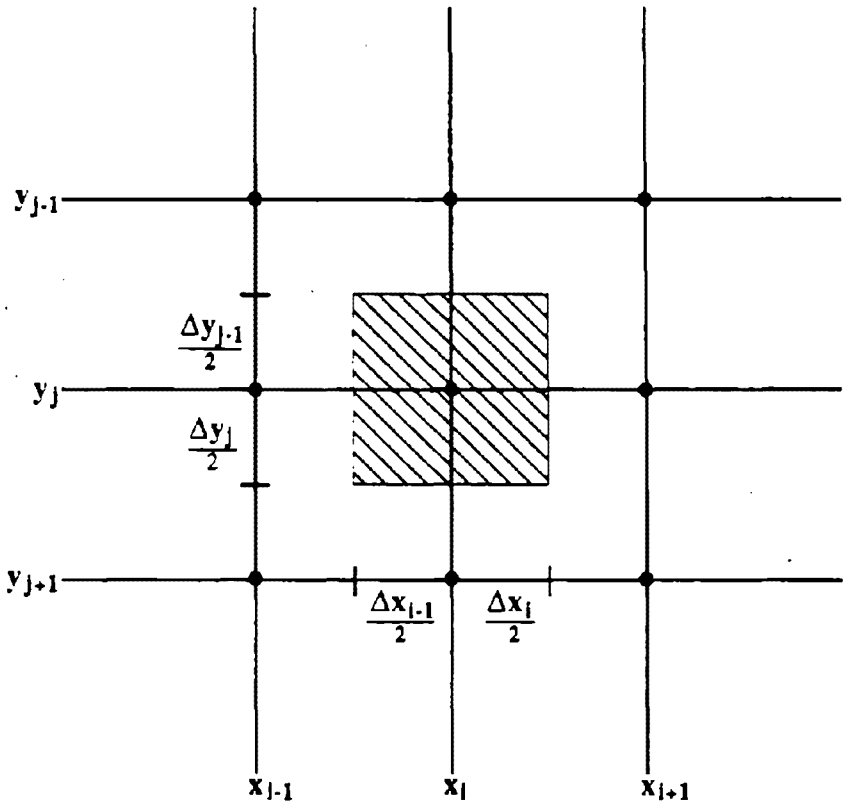

Figure 3. Local interior region of lattice points showing subregion D_{ij}.

We choose the integrated steady state hydraulic head field equation method developed by Varga (1962, pp. 181-191). The details of the development were given by Lindstrom and Boersma (1990). The following system of linear finite difference equations is obtained.

For $i = 1,2,\ldots N_x-1$, $j = 1,2,\ldots N_y-1$

$$a\ell t2_{i,j}\,\tilde{H}_{i-1,j} + adt1_{i,j}\,\tilde{H}_{i,j-1} + (adt2x_{i,j} + adt2y_{i,j})\,\tilde{H}_{i,j}$$

$$+ adt3_{i,j}\,\tilde{H}_{i,j+1} + aut2_{i,j}\,\tilde{H}_{i+1,j} = \left(\frac{Q_{inj} - Q_{out}}{\rho_w}\right)_{i,j}. \qquad (4.2.1)$$

where $\tilde{H}_{i,j}$ is the approximate hydraulic head evaluated at nodal point (x_i, y_j). The coefficients given in equation (4.2.1) are defined as follows:

$$a\ell t2_{i,j} = -\frac{\left(\dfrac{K_{sxx_{i-1/2,j}}}{\Delta x_{i-1}}\right)}{\left(\dfrac{\Delta x_{i-1} + \Delta x_i}{2}\right)}, \qquad (4.2.2)$$

$$adt1_{i,j} = -\frac{\left(\dfrac{K_{syy_{i,j-1/2}}}{\Delta y_{j-1}}\right)}{\left(\dfrac{\Delta y_{j-1} + \Delta y_j}{2}\right)}, \qquad (4.2.3)$$

$$adt2y_{i,j} = \frac{\left(\dfrac{K_{syy_{i,j+1/2}}}{\Delta y_j} + \dfrac{K_{syy_{i,j-1/2}}}{\Delta y_{j-1}}\right)}{\left(\dfrac{\Delta y_{j-1} + \Delta y_j}{2}\right)}, \qquad (4.2.4)$$

$$adt2x_{i,j} = \frac{\left(\dfrac{K_{sxx_{i+1/2,j}}}{\Delta x_i} + \dfrac{K_{sxx_{i-1/2,j}}}{\Delta x_{i-1}}\right)}{\left(\dfrac{\Delta x_{i-1} + \Delta x_i}{2}\right)}, \qquad (4.2.5)$$

$$adt3_{i,j} = -\frac{\left(\dfrac{K_{syy_{i,j+1/2}}}{\Delta y_j}\right)}{\left(\dfrac{\Delta y_{j-1} + \Delta y_j}{2}\right)}, \qquad (4.2.6)$$

$$aut2_{i,j} = -\frac{\left(\dfrac{K_{sxx_{i+1/2,j}}}{\Delta x_i}\right)}{\left(\dfrac{\Delta x_{i-1} + \Delta x_i}{2}\right)} . \tag{4.2.7}$$

Equations (4.2.2) through (4.2.7) show that the components of the hydraulic conductivity tensor are evaluated at mid-nodal points. The hydraulic conductivity field is not currently available at these points. However, the values of K_{sxx} and K_{syy} are known at all the nodal points of the domain $\bar{D}$. Because of the $C^{1,1}(\bar{D})$ smoothness of K_{sxx} and K_{syy} and the low order of the finite difference approximations to the first derivatives themselves, the arithmetic mean between adjacent nodal points is used as the approximation to the mid-nodal point values of K_{sxx} and K_{syy}

$$K_{sxx_{i+1/2,j}} \doteq \frac{K_{sxx_{i+1,j}} + K_{sxx_{i,j}}}{2} , \tag{4.2.8}$$

$$K_{sxx_{i-1/2,j}} \doteq \frac{K_{sxx_{i,j}} + K_{sxx_{i-1,j}}}{2} , \tag{4.2.9}$$

$$K_{syy_{i,j+1/2}} \doteq \frac{K_{syy_{i,j+1}} + K_{syy_{i,j}}}{2} , \tag{4.2.10}$$

$$K_{syy_{i,j-1/2}} \doteq \frac{K_{syy_{i,j}} + K_{syy_{i,j-1}}}{2} . \tag{4.2.11}$$

4.3. Boundary Conditions

Equations (4.1.4) and (4.1.5) are Dirichlet conditions, because the total hydraulic field along the planes $y = 0$ and $y = L_y$ is specified. Hence,

$$H(x,0) = H_{in}(x_i) = \tilde{H}(x_i,0), \qquad 0 \le x \le L_x. \tag{4.3.1}$$

Similarly at $y = L_y$ define

$$\tilde{H}_{i,Ny} = H_{out}(x_i), \qquad 0 \le x \le L_x. \tag{4.3.2}$$

Equations (4.1.6) and (4.1.7) are Neumann conditions, since the flux in the direction normal to the surface is specified. In this case, impermeable walls along the planes $x = 0$ and $x = L_x$ exist, so that a zero or no flux boundary condition obtains, i.e. along $x = 0$, where $\partial H/\partial x = 0$, approximate for $j = 1,2, N_{y-1}$,

$$\left.\frac{\partial H}{\partial x}\right|_{x=0} = 0 \doteq \left\{-\left(2 + \frac{\Delta x_2}{\Delta x_1}\right) \tilde{H}_{0,j} + \left(\frac{\Delta x_2}{\Delta x_1} + 2 + \frac{\Delta x_1}{\Delta x_2}\right) \tilde{H}_{1,j} - \frac{\Delta x_1}{\Delta x_2} \tilde{H}_{2,j}\right\} / (\Delta x_1 + \Delta x_2) , \tag{4.3.3}$$

a formula obtained by differentiating the Lagrange degree 2 interpolating polynomial,

$$P_2(x) = \tilde{H}_{0,j} + \left[\frac{\tilde{H}_{1,j} - \tilde{H}_{0,j}}{\Delta x_1}\right] (x - x_0) + \left[\frac{\dfrac{\tilde{H}_{2,j} - \tilde{H}_{1,j}}{\Delta x_2} - \dfrac{\tilde{H}_{1,j} - \tilde{H}_{0,j}}{\Delta x_1}}{\Delta x_1 + \Delta x_2}\right] (x - x_0)(x - x_0 - \Delta x_1) , \tag{4.3.4}$$

setting $x = x_c$ (=0) with $P_2'(x_0) = 0$, and simplifying the result. Since Δx_1 and Δx_2 are positive, possibly nonuniform nodal spacings, the definition of $H_{0,j}$ is obtained as a linear combination of $H_{1,j}$ and $H_{2,j}$:

$$\tilde{H}_{0,j} = \frac{\left(2 + \frac{\Delta x_2}{\Delta x_1} + \frac{\Delta x_1}{\Delta x_2}\right)\tilde{H}_{1,j} - \left(\frac{\Delta x_1}{\Delta x_2}\tilde{H}_{2,j}\right)}{\left(2 + \frac{\Delta x_2}{\Delta x_1}\right)} . \tag{4.3.5}$$

It can be shown in like manner that at $x = L_x$ where $\left.\frac{\partial H}{\partial x}\right|_{x=L_x} = 0$,

$$\tilde{H}_{Nx,j} = \frac{\left(\frac{-\Delta x_{Nx}}{\Delta x_{Nx-1}}\tilde{H}_{Nx-2,j}\right) + \left(2 + \frac{\Delta x_{Nx}}{\Delta x_{Nx-1}} + \frac{\Delta x_{Nx-1}}{\Delta x_{Nx}}\right)\tilde{H}_{Nx-1,j}}{\left(2 + \frac{\Delta x_{Nx-1}}{\Delta x_{Nx}}\right)} , \tag{4.3.6}$$

for $j = 1,2,\ldots N_y - 1$.

A standard Taylor series based error analysis leads to the errors:

$$\text{at } x = 0,\ O_1(\Delta x_1\ \Delta x_2) , \tag{4.3.7}$$

which if $\Delta x_1 = \Delta x_2 = \Delta x$ is $O_1(\Delta x^2)$ and

$$\text{at } x = L_x,\ O_2(\Delta x_{Nx}\ \Delta x_{Nx-1}) , \tag{4.3.8}$$

which if $\Delta x_{Nx} = \Delta x_{N-1} = \Delta x$ is $O_2(\Delta x^2)$.

It is good practice to choose Δx_1, Δx_2, Δx_{Nx-1}, and Δx_{Nx} equal to about 1/10 the intradomain node spacing of the lattice.

4.4. Solution of the Linear System of Equations

A vertical or horizontal ordering of the nodes may be chosen in equation (4.2.17). In either case, when using the boundary data, the system may be written in matrix form

$$A\,\underset{\sim}{\tilde{H}} = \underset{\sim}{b} , \tag{4.4.1}$$

where A is a real, nonsymmetric, N_x-1 • N_y-1 by N_x-1 • N_y-1, 5-band array which is irreducible, weakly diagonally dominant, and positive definite array, an M-array as defined by Varga (1962, pp. 186-188), and b is the vector of boundary data and source/sink data. $\tilde{\underset{\sim}{H}}$ then exists uniquely as

$$\tilde{\underset{\sim}{H}} = A^{-1} \underset{\sim}{b} \ . \tag{4.4.2}$$

Because storage requirements for a standard direct LU decomposition method are high, a rapidly converging robust iterative method was chosen for finding $\tilde{\underset{\sim}{H}}$. The method chosen is the Strongly Implicit Procedure (SIP) described by Stone (1968). A heuristic for choosing the "cancellation of terms" parameter is included in the SIP subroutine (Bachelor et al., 1990).

4.5. Velocity Components

Once all components of H are known, the x and y components of the Darcy fluid velocity field, and also the effective pore velocities, can be estimated using equation (4.1.1). However, since the hydraulic head field H(x,y) is known only approximately and only on a finite set of grid points, the two velocity components must be numerically estimated at each (x_i, y_j).

Two 3-point Lagrange polynomials, one in x and the other in y, similar to those stated by equation (4.3.4), are differentiated at the intranode points. Differentiation is done first along the x-coordinate to provide an estimate of $\partial H/\partial x|_{i,j}$ and then along the y-coordinate to provide an estimate of $\partial H/\partial y|_{i,j}$. For the nodes inside Đ and adjacent to the impervious walls as well as those nodes inside Đ but adjacent to

the inlet and outlet boundaries, velocity estimates are obtained using the formulas:

at $y = 0$, for $i = 1,2,\ldots N_{x-1}$,

$$\left.\frac{\partial H}{\partial y}\right|_{y=0} \doteq \frac{\tilde{H}_{i,1} - \tilde{H}_{i,0}}{\Delta y_1}, \tag{4.5.1}$$

$$\left.\frac{\partial H}{\partial x}\right|_{y=0} \doteq -\frac{\Delta x_i}{\Delta x_{i-1}(\Delta x_{i-1} + \Delta x_i)} \tilde{H}_{i-1,0} + \left(\frac{1}{\Delta x_{i-1}} - \frac{1}{\Delta x_i}\right) \tilde{H}_{i,0} + \frac{\Delta x_{i-1}}{\Delta x_i(\Delta x_{i-1} + \Delta x_i)} \tilde{H}_{i+1,0}, \tag{4.5.2}$$

at $y = L_y$, for $i = 1,2,\ldots N_{x-1}$,

$$\left.\frac{\partial H}{\partial y}\right|_{y=L_y} \doteq \frac{\tilde{H}_{i,Ny} - \tilde{H}_{i,Ny-1}}{\Delta y_{Ny}}, \tag{4.5.3}$$

$$\left.\frac{\partial H}{\partial x}\right|_{y=L_y} \doteq -\frac{\Delta x_i}{\Delta x_{i-1}(\Delta x_{i-1} + \Delta x_i)} \tilde{H}_{i-1,Ny} + \left(\frac{1}{\Delta x_{i-1}} - \frac{1}{\Delta x_i}\right) \tilde{H}_{i,Ny} + \frac{\Delta x_{i-1}}{\Delta x_i(\Delta x_{i-1} + \Delta x_i)} \tilde{H}_{i+1,Ny}, \tag{4.5.4}$$

at $x = 0$, for $j = 1,2,\ldots N_y - 1$

$$\left.\frac{\partial H}{\partial x}\right|_{x=0} = 0, \text{ according to equation (4.1.6)}, \tag{4.5.5}$$

$$\left.\frac{\partial H}{\partial y}\right|_{x=0} \doteq -\frac{\Delta y_j}{\Delta y_{j-1}(\Delta y_{j-1} + \Delta y_j)} \tilde{H}_{0,j-1}$$

$$+ \left(\frac{1}{\Delta y_{j-1}} - \frac{1}{\Delta y_j}\right) \tilde{H}_{0,j}$$

$$+ \frac{\Delta x_{j-1}}{\Delta y_j(\Delta y_{j-1} + \Delta y_j)} \tilde{H}_{0,j+1} , \qquad (4.5.6)$$

at $x = L_x$, for $j = 1,2,\ldots N_{y-1}$

$$\left.\frac{\partial H}{\partial x}\right|_{x=L_x} = 0, \text{ according to equation (4.1.7)}, \qquad (4.5.7)$$

$$\left.\frac{\partial H}{\partial y}\right|_{x=L_x} \doteq -\frac{\Delta y_j}{\Delta y_{j-1}(\Delta y_{j-1} + \Delta y_j)} \tilde{H}_{Nx,j-1}$$

$$+ \left(\frac{1}{\Delta y_{j-1}} - \frac{1}{\Delta y_j}\right) \tilde{H}_{Nx,j}$$

$$+ \frac{\Delta y_{j-1}}{\Delta y_j(\Delta y_{j-1} + \Delta y_j)} \tilde{H}_{Nx,j+1} . \qquad (4.5.8)$$

For the remainder of the internal nodes write:

$$\left.\frac{\partial H}{\partial x}\right|_{(x_i,y_j)} \doteq -\frac{\Delta x_i}{\Delta x_{i-1}(\Delta x_{i-1} + \Delta x_i)} \tilde{H}_{i-1,j}$$

$$+ \left(\frac{1}{\Delta x_{i-1}} - \frac{1}{\Delta x_i}\right) \tilde{H}_{i,j}$$

$$+ \frac{\Delta x_{i-1}}{\Delta x_i(\Delta x_{i-1} + \Delta x_i)} \tilde{H}_{i+1,j}, \qquad (4.5.9)$$

and

$$\left.\frac{\partial H}{\partial y}\right|_{(x_i,y_j)} \doteq -\frac{\Delta y_j}{\Delta y_{j-1}(\Delta y_{j-1}+\Delta y_j)}\tilde{H}_{i,j-1}$$

$$+\left(\frac{1}{\Delta y_{j-1}}-\frac{1}{\Delta y_j}\right)\tilde{H}_{i,j}$$

$$+\frac{\Delta y_{j-1}}{\Delta y_j(\Delta y_{j-1}+\Delta y_j)}\tilde{H}_{i,j+1}\ . \qquad (4.5.10)$$

Formulas (4.5.1) and (4.5.3) which approximate $\partial H/\partial y$ along the open portions at $y = 0$ and $y = L_y$ are $O(\Delta y)$ and $O(\Delta y_{N_y})$ accurate. The remaining approximations are $O(\Delta x_i\ \Delta x_{i-1})$ and $O(\Delta y_j\ \Delta y_{j-1})$ accurate. These results are easily confirmed by means of standard Taylor series analysis. Close to the walls, at the inlet and exit ports, and near the injection and extraction wells, the nodal spacing must be chosen to be very small for accurate approximations. In preliminary work it has been found experimentally that to obtain U_x and U_y to three or four significant digits, $H(x,y)$ must be computed to about eight significant digits. This is so because of the loss of significant digits which occurs with numerical differentiation of tabular data.

5. CHEMICAL TRANSPORT AND FATE MODEL

5.1. Transport and Fate Equations

This section describes the basic equations for chemical transport and fate in the single layer aquifer. The assumptions, which form the basis for the transport and fate model and which hold for each one of the four chemical compounds, i.e. substrate, S; nutrient, Nu; oxygen, O; and Nitrate, Ni, are now listed.

1) Mass transport is via advection (convection) and dispersion.

2) The x and y dispersion components are linearly dependent upon the moduli of the velocity components of the flow field for two-dimensional flow in an isotropic and nonhomogeneous aquifer (Bear and Verruijt, 1987, p. 161-164)

$$D^*_{xx} = \alpha_{tort} D^*_{L\phi} + \alpha^*_{dispy} \frac{(U_x)^2}{|\underset{\sim}{U}|} + \alpha^*_{dispx} \frac{(U_y)^2}{|\underset{\sim}{U}|} \tag{5.1.1}$$

and

$$D^*_{yy} = \alpha_{tort} D^*_{L\phi} + \alpha^*_{dispx} \frac{(U_x)^2}{|\underset{\sim}{U}|} + \alpha^*_{dispy} \frac{(U_y)^2}{|\underset{\sim}{U}|}, \tag{5.1.2}$$

where the magnitude of the local seepage velocity vector U is defined by

$$|\underset{\sim}{U}| = \left[(U_x)^2 + (U_y)^2\right]^{1/2} , \tag{5.1.3}$$

and the longitudinal axis coincides with the y-axis (Konikow and Bredehoeft, 1978). The cross-axis dispersion coefficient D_{xy} is symmetrical so that $D_{yx} = D_{xy}$ and

$$D^*_{xy} = [\alpha^*_{dispy} - \alpha^*_{dispx}] \frac{U_x U_y}{|\underset{\sim}{U}|} , \tag{5.1.4}$$

where the * superscript denotes any one of the four dissolved chemicals. The convention for this superscript is that once a chemical symbol is chosen, it is thereafter consistently substituted for the symbol * unless otherwise stated. The longitudinal and transverse dispersivities (α^*_{dispy}, α^*_{dispx}) as well as the tortuosity (α_{tort}) are assumed to be once continuously differentiable functions of x and y inside the flow domain Đ.

3) The porous medium can be partitioned into three distinct fractions as follows:

i) sorbing particles (clay minerals and small silt particles),

ii) weakly sorbing particles (large silt and sand particles), and

iii) strongly sorbing organic matter,

with the following linear equilibrium sorption rule assumed to hold for the porous medium

$$S^* = (M_{ws}/M_t\ \rho_{ws}\ K^*_{ws} + M_s/M_t\ \rho_s\ K^*_s + M_o/M_t\ \rho_{org}\ K^*_{org})C^* \quad . \tag{5.1.5}$$

The assumed linear equilibrium sorption rule of equation (5.1.5) gives rise to the set of retention coefficients (Lindstrom et al., 1989)

$$R^* = \frac{1 - \epsilon}{\epsilon}\ ((M_{ws}/M_t)\ \rho_{ws}\ K^*_{ws} + (M_s/M_t)\ \rho_s\ K^*_s + (M_o/M_t)\ \rho_{org}\ K^*_{org}) \quad . \tag{5.1.6}$$

The three porous medium fractions (M_{ws}/M_t, M_sM_t, M_o/M_t) are continuous functions of x and y in Đ.

4) Chemicals can be introduced into the aquifer with the feed stream at the inlet end (y = 0) or from constantly emitting sources in the aquifer. Fluids added by these methods must have a low volumetric concentration and the flow rates must be low enough so that the previously established fluid flow field is not disturbed. It is assumed that density gradients, density stratification, or local changes in the transport and/or fate properties of the porous medium do not occur in time.

5) Water containing chemicals can be introduced via fully penetrating injection wells or extracted from similar wells by pumping.

6) Loss of chemical can occur via first order irreversible loss processes such as chemical transformations and precipitation in both the free and sorbed phases in addition to loss via microbial degradation. The overall first order irreversible process law for each chemical is characterized by the constant

$$\Lambda^* = \lambda^*_{irr} + R^*_{irr}\,\lambda^* \,. \tag{5.1.7}$$

All the first order loss process coefficients are assumed to be continuous functions of x and y inside Đ.

7) Microbiological processes are modeled using process laws described by Molz et al. (1986) and Widdowson et al. (1988), who constructed biodegradation models using the carbon assimilation and oxidation assumptions of Herbert (1958). The model developed here includes two microbial populations, namely $N_1(t)$ (number of cells per kg of dry soil), which utilizes substrate under both aerobic and anaerobic conditions, and $N_2(t)$ (number of cells per kg of dry soil), which utilizes substrate only under aerobic conditions. The utilization rate laws adapted from Widdowson et al. (1988) are

$$r^1_{sonu} = \frac{\mu^1_o}{Y^1_{so}}\left(\frac{C^s}{K^1_{so} + C^s}\right)\left(\frac{C^o}{K^1_o + C^o}\right)\left(\frac{C^{nu}}{K^1_{onu} + C^{nu}}\right) , \tag{5.1.8}$$

$$r^2_{sonu} = \frac{\mu^2_o}{Y^2_{so}}\left(\frac{C^s}{K^2_{so} + C^s}\right)\left(\frac{C^o}{K^2_o + C^o}\right)\left(\frac{C^{nu}}{K^2_{onu} + C^{nu}}\right) , \tag{5.1.9}$$

$$r^1_{sninu} = \frac{\mu^1_n}{Y^1_{sni}} \left(\frac{C^s}{K^1_{sni} + C^s}\right)\left(\frac{C^{ni}}{K^1_{ni} + C^{ni}}\right)\left(\frac{C^{nu}}{K^1_{ninu} + C^{nu}}\right)\left(1 + \frac{C^o}{K^1_{oni}}\right)^{-1} , \quad (5.1.10)$$

where the units of r are (kg kg^{-1} day^{-1}). The growth of the two microbial populations adapted from Widdowson et al. (1988) are

$$\frac{\partial N_1}{\partial t} = [(Y^1_{so}\ r^1_{sonu} - \delta^1) + Y^1_{sni}\ r^1_{sninu}]\ N_1, \quad N_1(0) = N_{10}(\geq 0) , \quad (5.1.11)$$

$$\frac{\partial N_2}{\partial t} = [(Y^2_{so}\ r^2_{sonu} - \delta^2]N_2, \quad N_2(0) = N_{20}(\geq 0) . \quad (5.1.12)$$

The two maintenance rate coefficients δ^1 and δ^2 at time t = 0 are defined by

$$\delta^1 = (Y^1_{so}\ r^1_{sonu} + Y^1_{sni}\ r^1_{sninu})_{t=0} , \quad (5.1.13)$$

$$\delta^2 = (Y^2_{so}\ r^2_{sonu})_{t=0} . \quad (5.1.14)$$

Consideration of the balance of chemical mass in the REV leads to the coupled system of four nonlinear, two-dimensional, transport and fate equations.

<u>Nutrient</u>

$$V_{REV}\ \epsilon(1 + R^{nu})\ \frac{\partial C^{nu}}{\partial t} = V_{REV} \left\{\frac{\partial}{\partial x} (\epsilon\ D^{nu}_{xx} \frac{\partial C^{nu}}{\partial x})\right.$$

$$+ \frac{\partial}{\partial x} (\epsilon\ D^{nu}_{xy} \frac{\partial C^{nu}}{\partial y}) + \frac{\partial}{\partial y} (\epsilon\ D^{nu}_{yx} \frac{\partial C^{nu}}{\partial x}) + \frac{\partial}{\partial y} (\epsilon\ D^{nu}_{yy} \frac{\partial C^{nu}}{\partial y})$$

$$\left. - \frac{\partial}{\partial x} (\epsilon\ U_x\ C^{nu}) - \frac{\partial}{\partial y} (\epsilon\ U_y\ C^{nu})\right\}$$

$$- V_{REV}\ \rho_b((\psi^1_o\ r^1_{sonu} + \theta^1_{ni}\ r^1_{sninu})\ N_1(x,y,t)$$

$$+ \psi_o^2 \, r^2_{sonu} \, N_2(x,y,t)) + V_{REV}(Q_{inj} \, C^{nu}_{sour} + Q^{nu}_{so}$$

$$- \frac{Q_{out}}{\rho_w} C^{nu} - \epsilon \, \Lambda^{nu} \, C^{nu}) \; . \qquad (5.1.15)$$

Substrate

$$V_{REV} \, \epsilon(1 + R^s) \frac{\partial C^s}{\partial t} = V_{REV} \left\{ \frac{\partial}{\partial x} (\epsilon \, D^s_{xx} \frac{\partial C^s}{\partial x}) \right.$$

$$+ \frac{\partial}{\partial x} (\epsilon \, D^s_{xy} \frac{\partial C^s}{\partial y}) + \frac{\partial}{\partial y} (\epsilon \, D^s_{yx} \frac{\partial C^s}{\partial x}) + \frac{\partial}{\partial y} (\epsilon \, D^s_{yy} \frac{\partial C^s}{\partial y})$$

$$\left. - \frac{\partial}{\partial x} (\epsilon \, U_x \, C^s) - \frac{\partial}{\partial y} (\epsilon \, U_y \, C^s) \right\}$$

$$- V_{REV} \, \rho_b((r^1_{sonu} + r^1_{sninu}) \, N_1(x,y,t)$$

$$+ r^2_{sonu} \, N_2(x,y,t)) + V_{REV}(Q_{inj} \, C^s_{sour} + Q^s_{so}$$

$$- \frac{Q_{out}}{\rho_w} C^s - \epsilon \, \Lambda^s \, C^s) \; . \qquad (5.1.16)$$

Oxygen

$$V_{REV} \, \epsilon(1 + R^o) \frac{\partial C^o}{\partial t} = V_{REV} \left\{ \frac{\partial}{\partial x} (\epsilon \, D^o_{xx} \frac{\partial C^o}{\partial x}) \right.$$

$$+ \frac{\partial}{\partial x} (\epsilon \, D^o_{xy} \frac{\partial C^o}{\partial y}) + \frac{\partial}{\partial y} (\epsilon \, D^o_{yx} \frac{\partial C^o}{\partial x}) + \frac{\partial}{\partial y} (\epsilon \, D^o_{yy} \frac{\partial C^o}{\partial y})$$

$$\left. - \frac{\partial}{\partial x} (\epsilon \, U_x \, C^o) - \frac{\partial}{\partial y} (\epsilon \, U_y \, C^o) \right\}$$

$$- V_{REV} \, \rho_b \left\{ (\gamma^1_o \, r^1_{sonu} + \alpha^1_o \, \delta^1 \frac{C^o}{K^1_{som} + C^o}) \, N_1(x,y,t) \right.$$

$$+ \left(\gamma_o^2 \, r_{sonu}^2 + \alpha_o^2 \, \delta^2 \frac{C^o}{K_{som}^2 + C^o}\right) N_2(x,y,t)\Big\}$$

$$+ V_{REV}\left(Q_{inj} \, C_{sour}^o + Q_{so}^o - \frac{Q_{out}}{\rho_w} C^o - \epsilon \, \Lambda^o \, C^o\right) . \qquad (5.1.17)$$

<u>Nitrate</u>

$$V_{REV} \, \epsilon(1 + R^{ni}) \frac{\partial C^{ni}}{\partial t} = V_{REV} \Big\{\frac{\partial}{\partial x}\left(\epsilon \, D_{xx}^{ni} \frac{\partial C^{ni}}{\partial x}\right)$$

$$+ \frac{\partial}{\partial x}\left(\epsilon \, D_{xy}^{ni} \frac{\partial C^{ni}}{\partial y}\right) + \frac{\partial}{\partial y}\left(\epsilon \, D_{yx}^{ni} \frac{\partial C^{ni}}{\partial x}\right) + \frac{\partial}{\partial y}\left(\epsilon \, D_{yy}^{ni} \frac{\partial C^{ni}}{\partial y}\right)$$

$$- \frac{\partial}{\partial x}\left(\epsilon \, U_x \, C^{ni}\right) - \frac{\partial}{\partial y}\left(\epsilon \, U_y \, C^{ni}\right)\Big\}$$

$$- V_{REV} \, \rho_b \Big\{\left(\eta_{ni}^1 \, r_{sninu}^1 + \alpha_{ni}^1 \, \delta^1 \left[\frac{C^{ni}}{K_{ni}^1 + C^{ni}}\right]\left[\frac{1}{1 + \frac{C^o}{K_{oni}^1}}\right]\right) N_1(x,y,t)\Big\}$$

$$+ V_{REV}\left(Q_{inj} \, C_{sour}^{ni} + Q_{so}^{ni} - \frac{Q_{out}}{\rho_w} C^{ni} - \epsilon \, \Lambda^{ni} \, C^{ni}\right) . \qquad (5.1.18)$$

The advection terms in equations (5.1.15) through (5.1.18) can be simplified by using the relationship

$$\frac{\partial(\epsilon U_x)}{\partial x} + \frac{\partial(\epsilon U_y)}{\partial y} = \frac{Q_{inj} - Q_{out}}{\rho_w}$$

from equation (4.1.3) in each of the four transport and fate equations. Since V_{REV} is nonzero, both sides of equations (5.1.15) through (5.1.18) can be divided by V_{REV}. This yields the generic transport and fate equation:

$$\frac{\partial C^*}{\partial t} + U_x^* \frac{\partial C^*}{\partial x} + U_y^* \frac{\partial C^*}{\partial y} + \left(\frac{\Lambda^*}{1 + R^*}\right) C^* + \frac{\lambda^*(x,y,t)}{1 + R^*}$$

$$= \left\{\frac{\partial}{\partial x}\left(\epsilon D_{xx}^* \frac{\partial C^*}{\partial x}\right) + \frac{\partial}{\partial x}\left(\epsilon D_{xy}^* \frac{\partial C^*}{\partial y}\right)\right.$$

$$\left. + \frac{\partial}{\partial y}\left(\epsilon D_{yx}^* \frac{\partial C^*}{\partial x}\right) + \frac{\partial}{\partial y}\left(\epsilon D_{yy}^* \frac{\partial C^*}{\partial y}\right)\right\} / [(\epsilon(1 + R^*))]$$

$$+ \frac{Q_{so}^* + Q_{inj}(C_{sour}^* - \frac{C^*}{\rho_w})}{\epsilon(1 + R^*)} , \qquad (5.1.19)$$

where

$$U_x^* = \frac{U_x}{1 + R^*} \quad \text{and} \quad U_y^* = \frac{U_y}{1 + R^*} , \qquad (5.1.20)$$

and $\lambda^*_{(x,y,t)}$ is the loss rate function due to microbial processes operating at point (x,y,t) in the space-time cylinder $D^* = D \cup [0,T]$. The $\lambda^*_{(x,y,t)}$ for each chemical is:

<u>nutrient</u>

$$\lambda^{nu}(x,y,t) = \rho_b \{(\psi_o^1 r_{sonu}^1 + \theta_{ni}^1 r_{sninu}^1) N_1(x,y,t)$$

$$+ \psi_o^2 r_{sonu}^2 N_2(x,y,t)\} / \epsilon , \qquad (5.1.21)$$

<u>substrate</u>

$$\lambda^s(x,y,t) = \rho_b\{(r_{sonu}^1 + r_{sninu}^1) N_1(x,y,t) + r_{sonu}^2 N_2(x,y,t)\}/\epsilon , \qquad (5.1.22)$$

oxygen

$$\lambda^{o}(x,y,t) = \rho_b \left\{ \left[\gamma_o^1 \, r_{sonu}^1 + \alpha_o^1 \, \delta^1 \left(\frac{C^o}{K_{som}^1 + C^o} \right) \right] N_1(x,y,t) \right.$$

$$\left. + \left[\gamma_o^2 \, r_{sonu}^2 + \alpha_o^2 \, \delta^2 \, \frac{C^o}{K_{som}^2 + C^o} \right] N_2(x,y,t) \right\} / \epsilon \, , \qquad (5.1.23)$$

nitrate

$$\lambda^{ni}(x,y,t) = \rho_b \left\{ (\eta_{ni}^1 \, r_{sninu}^1 \right.$$

$$\left. + \alpha_{ni}^1 \, \delta^1 \left(\frac{C^{ni}}{K_{ni}^1 + C^{ni}} \right) \left(\frac{K_{oni}^1}{K_{oni}^1 + C^o} \right) \right\} N_1(x,y,t) \, / \, \epsilon \, . \qquad (5.1.24)$$

Since the "effective" material or total derivative $\frac{d\,C^*}{dt}$ is

$$\frac{d\,C^*}{dt} = \frac{\partial C^*}{\partial t} + U_x^* \frac{\partial C^*}{\partial x} + U_y^* \frac{\partial C^*}{\partial y} \, ,$$

substitution in equation (5.1.19) obtains

$$\frac{dC^*}{dt} + \left(\frac{\Lambda^*}{1 + R^*} \right) C^* + \frac{\lambda^*(x,y,t)}{1 + R^*}$$

$$= \left\{ \frac{\partial}{\partial y} \left(\epsilon \, D_{xx}^* \frac{\partial C^*}{\partial x} \right) + \frac{\partial}{\partial x} \left(\epsilon \, D_{xy}^* \frac{\partial C^*}{\partial y} \right) \right.$$

$$\left. + \frac{\partial}{\partial y} \left(\epsilon \, D_{yx}^* \frac{\partial C^*}{\partial x} \right) + \frac{\partial}{\partial y} \left(\epsilon \, D_{yy}^* \frac{\partial C^*}{\partial y} \right) \right\} / \, [\epsilon(1 + R^*)]$$

$$+ \{ Q_{so}^* + Q_{inj} (C_{sour}^* - \frac{C^*}{\rho_w}) \} \, / \, [\epsilon(1 + R^*)] \qquad (5.1.25)$$

as the generic transport and fate equation. This equation is used to describe the transport and fate of each compound in the aquifer. Closed form solutions such as combinations of elementary functions or eigen-

functions do not exist for the system of equations implied by equation (5.1.25). Therefore an approximate solution must be obtained using numerical procedures. The procedure used here is a type of finite difference Euler-Lagrange procedure (Cheng et al., 1984; Baptista et al., 1984; Baptista, 1986; Baptista, 1987), which is a modification of the method of characteristics. Equation (5.1.25) was written in the mixed Euler-Lagrange form in anticipation of choosing this method of approximation.

5.2. Initial Data, Boundary Data, and Total Chemical Mass

Completion of the conditions on C^* over the space-time cylinder D^* requires C^* to be prescribed at time $t = 0$, i.e.,

$$C^*(x,y,o^+) = g^*(x,y) \ , \tag{5.2.1}$$

where (x,y) is in D so that

$$L_w \int_D \int C^* \ (x,y,o^+)dxdy < \infty \ . \tag{5.2.2}$$

Equation (5.2.2) holds for each of the four chemicals.

Recall from Figure 2 that at each of the two planes $y = 0$ and $y = L_y$ the total hydraulic head is prescribed rather than the fluid fluxes. The fluid velocity field can vary across these planes, depending upon the presence or absence of injection and/or extraction wells in the interior. The chemical mass in the system is also desired. A complete accounting of all the chemical mass which enters and exits the aquifer via the inlet and outlet ports is required for each chemical. Fixing $C^*(x,o,t)$ and $C^*(x,L_y,t)$, $0 < x < L_x$, for all time $t > 0$ will not satisfy the accounting condition (Parker and van Genuchten, 1984). Furthermore, attempting to fix the concentration at $y = L_y$ is not possible in most

situations. In order to satisfy the mass accounting requirement, a flux type concept along the inlet and exit port boundaries is introduced. This concept allows conservation of mass better than would be possible by fixing the chemical concentrations at the inlet and exit port. Figures 4 and 5 show aspects of this concept of the mass conserving boundary conditions at the inlet and exit ports.

A detailed discussion of the development of the mass accounting boundary conditions at the inlet and outlet ports, induced by the finite size of the ports, was given by Lindstrom and Boersma (1990) for a single dissolved chemical. Thin boundary layers are introduced at each of the porous medium inlet and outlet port interfaces. Assuming that the four dissolved chemicals are noninteracting in either the inlet or exit ports, the inlet and outlet port concepts presented by Lindstrom and Boersma (1990) for one compound can be used for each of the four compounds. The boundary conditions at the inlet and outlet ports can then be written as

$$C^*(x,0,t) \doteq \frac{(\epsilon\, D^*_{yy})\Big|_{y=0} \dfrac{C^*(x,\Delta y_1,t)}{\Delta y_1} + \left[\dfrac{D^*_{cin}}{\Delta y_{in}} + (\epsilon\, U_y)_{y=0}\right] C^*_{in}}{\left[\dfrac{(\epsilon\, D^*_{yy})_{y=0}}{\Delta y_1} + (\epsilon\, U_y)_{y=0}\right] + \dfrac{D^*_{cin}}{\Delta y_{in}}} \tag{5.2.3}$$

and

$$C^*(x,L_y,t) = \frac{\left[\epsilon\, U_y + \dfrac{D^*_{yy}}{\Delta y_{Ny}}\right]_{y=L_y} C^*(x,L_y - \Delta y,t) + \dfrac{D^*_{cout}}{\Delta y_{out}} C^*_{out}}{\left[\epsilon\, U_y + \dfrac{\epsilon\, D^*_{yy}}{\Delta y_{Ny}}\right]_{y=L_y} + \dfrac{D^*_{cout}}{\Delta y_{out}}} \quad . \tag{5.2.4}$$

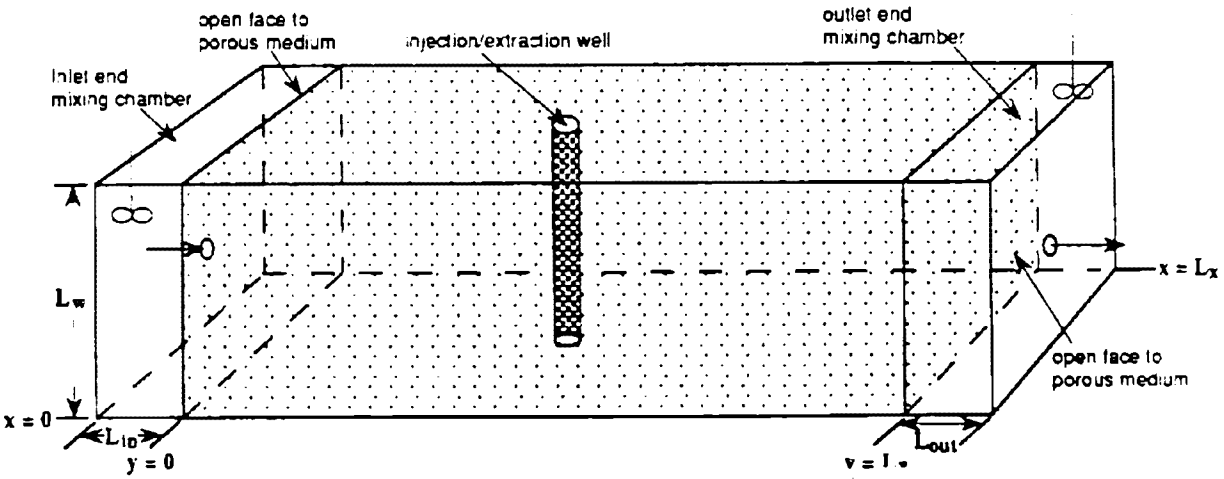

Figure 4. Schematic diagram of the physical aquifer used for testing the mathematical model, showing mixing chambers at inlet and outlet ends.

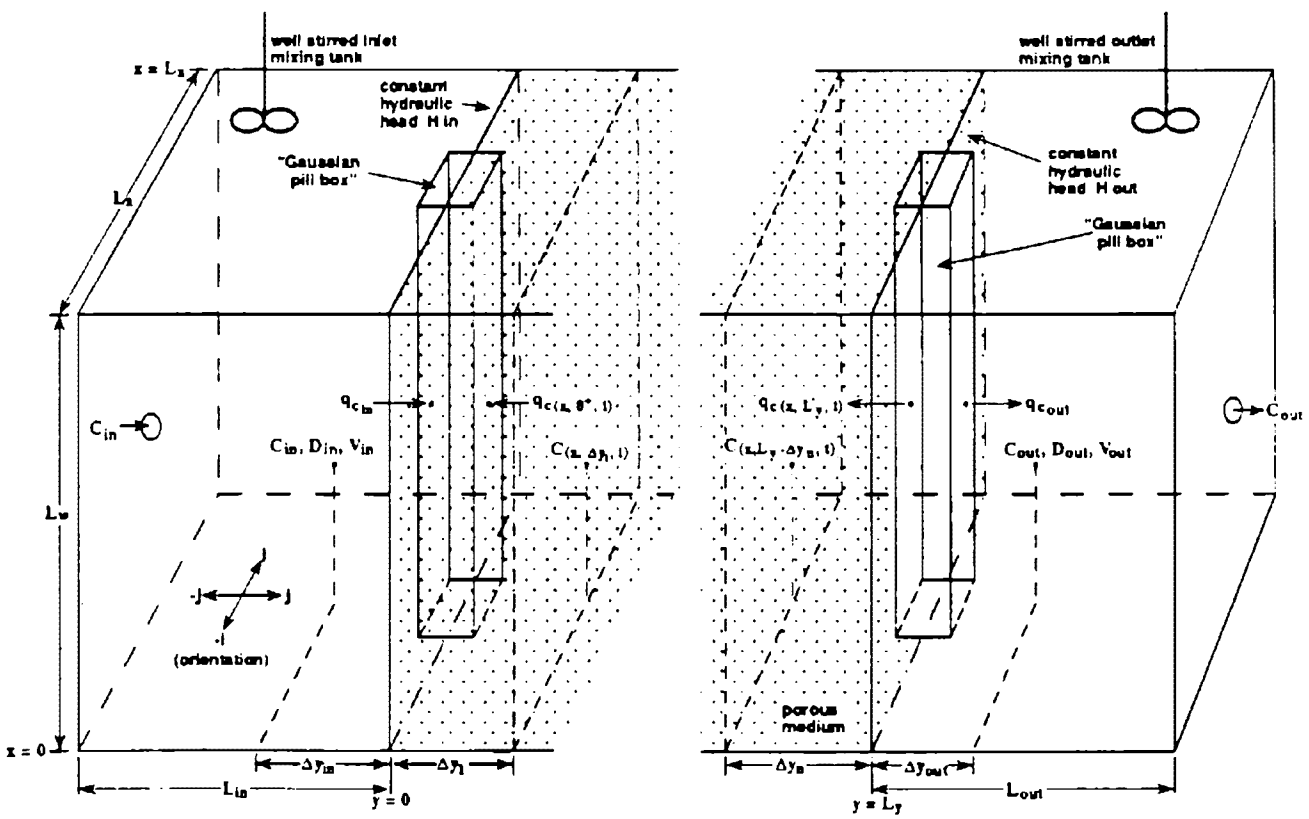

Figure 5. Details of the use of the "Gaussian pill box" concept in the mixing chambers, showing flow orientation, and positions where mathematical terms were defined.

It is easily seen from these two equations that in the limit as D^*_{cin} and $D^*_{cout} \rightarrow$ large, then $C^*(x,0,t) \rightarrow C^*_{in}$ and $C^*(x,L_y,t) \rightarrow C^*_{out}$, i.e. with the assumption of well stirred conditions in both the inlet and outlet chambers, the diffusion gradients within the ports themselves vanish.

The differential equations defining C^*_{in} and C^*_{out} were derived in detail by Lindstrom and Boersma (1990). They find that at the inlet port

$$\frac{dC^*_{in}}{dt} = C^*_o \frac{1}{L_{in}L_x} \int_0^{L_x} (\epsilon_y U)_{y=0} dx + \frac{1}{L_{in}L_x} \int_0^{L_x} \left.\frac{\epsilon D^*_{yy}}{\Delta y_1}\right|_{y=0} C^*(x,\Delta y_1,t)dx$$

$$- \frac{1}{L_{in}L_x} \left\{ \int_0^{L_x} \left[\frac{\epsilon D^*_{yy}}{\Delta y_1} + \epsilon U_y\right]_{y=0} dx \right\} C^*_{in} , \qquad (5.2.5)$$

and at the outlet port

$$\frac{dC^*_{out}}{dt} = \frac{1}{L_{out}L_x} \int_0^{L_x} \left[\left(\frac{\epsilon D^*_{yy}}{\Delta y_{Ny}} + \epsilon U_y\right)_{y=L_y} C^*(x,L_y - \Delta y_{Ny},t)\right] dx$$

$$- \frac{1}{L_{out} L_x} \left\{ \int_0^{L_x} \left(\frac{\epsilon D^*_{yy}}{\Delta y_{Ny}} + \epsilon U_y\right)_{y=L_y} dx \right\} C^*_{out} , \qquad (5.2.6)$$

where C^*_{in} and C^*_{out} at time $t = 0$ must be specified.

Along the planes $x = 0$ and $x = L_x$ the zero chemical flux (Neumann) conditions

$$\left.\frac{\partial C^*}{\partial x}\right|_{x=0} = 0 = \left.\frac{\partial C^*}{\partial x}\right|_{x=L_x} \qquad (5.2.7)$$

are required. These two conditions obtain directly from applying a Gaussian pill box concept to the impervious, bounding, walls and recalling that $U_x = 0$, along both walls as well.

The total chemical mass in the system at time t (days) following initiation of the transport and fate processes is defined by

$$M^*_{Aq}(t) = L_w \int_0^{L_y} \int_0^{L_x} \epsilon(1 + R^*)\, C^*(x,y,t)dxdy \ , \qquad (5.2.8)$$

where L_w is the vertical dimension (m) of the aquifer.

The total cumulative chemical mass entering (+) or leaving (-) the inlet port is defined by equation (5.2.9),

$$M^*_{inlet}(t) = L_w \int_0^{t} \int_0^{L_x} (\underset{\sim}{q}^*_c) \Big|_{y=0} \bullet (-\hat{j})dxdt \ . \qquad (5.2.9)$$

The total cumulative chemical mass leaving (+) or entering (-), the exit port is defined by equation (5.2.10),

$$M^*_{outlet}(t) = L_w \int_0^{t} \int_0^{L_x} (-\hat{j} \bullet -\underset{\sim}{q}^*_c \Big|_{y=L_y})dxdt \ . \qquad (5.2.10)$$

The total cumulative chemical mass "lost" by all first-order processes operating in the system is defined by equation (5.2.11),

$$M^*_{lost}(t) = L_w \int_0^{t} \int_0^{L_y} \int_0^{L_x} \{\epsilon^* \Lambda^* C(x,y,\tau) + \frac{Q_{out}\, C^*}{\rho_w}\}dxdyd\tau. \qquad (5.2.11)$$

The total cumulative chemical mass gained from distributed zero order sources, e.g. leaking sources, is defined by

$$M^*_{source}(t) = L_w \int_0^{t} \int_0^{L_y} \int_0^{L_x} \{Q^*_{SO}(x,y,\tau) + Q_{inj}\, C^*_s\}dxdyd\tau \ . \qquad (5.2.12)$$

The five scalar mass quantities, which are computed in the model LT3VSI give a complete mass accounting for the aquifer.

5.3. Approximate Solution for the Transport and Fate Equations

The approximation is initiated by recalling the subregion in space $Đ_{ij} \cup Đ$, which contains the i,jth nodal point of both the flow field and the chemical transport field (Figure 3). The time coordinate [0,T] is partitioned into a set of adjoining time subintervals so that time $t_n = t_{n-1} + \Delta t_n$, $n = 1,2,3,\ldots N_{max}$. Define

$$Đ^*_{ij} = Đ_{ij} \cup [0,T) \tag{5.3.1}$$

to be a space-time subcylinder so that

$$Đ^* = \bigcup_{i,j} \{Đ^*_{ij}\} \tag{5.3.2}$$

is the global space-time cylinder. Then,

$$Đ^*_{(n,n+1)} = \bigcup_{i,j} \{Đ_{ij} \cup (t_n, t_{n+1})\} \tag{5.3.3}$$

is that portion of $Đ^*$ made up of the generators of the space-time cylinder lying between the two planes $t = t_n$ and $t = t_{n+1}$. The objective is to set up the domain for a two time level computing procedure in anticipation of choosing an explicit and conditionally stable method, such as a "forward Euler" time integrator. Figure 6 shows a schematic diagram of the region of interest in $Đ^*_{ij(n,N+1)}$.

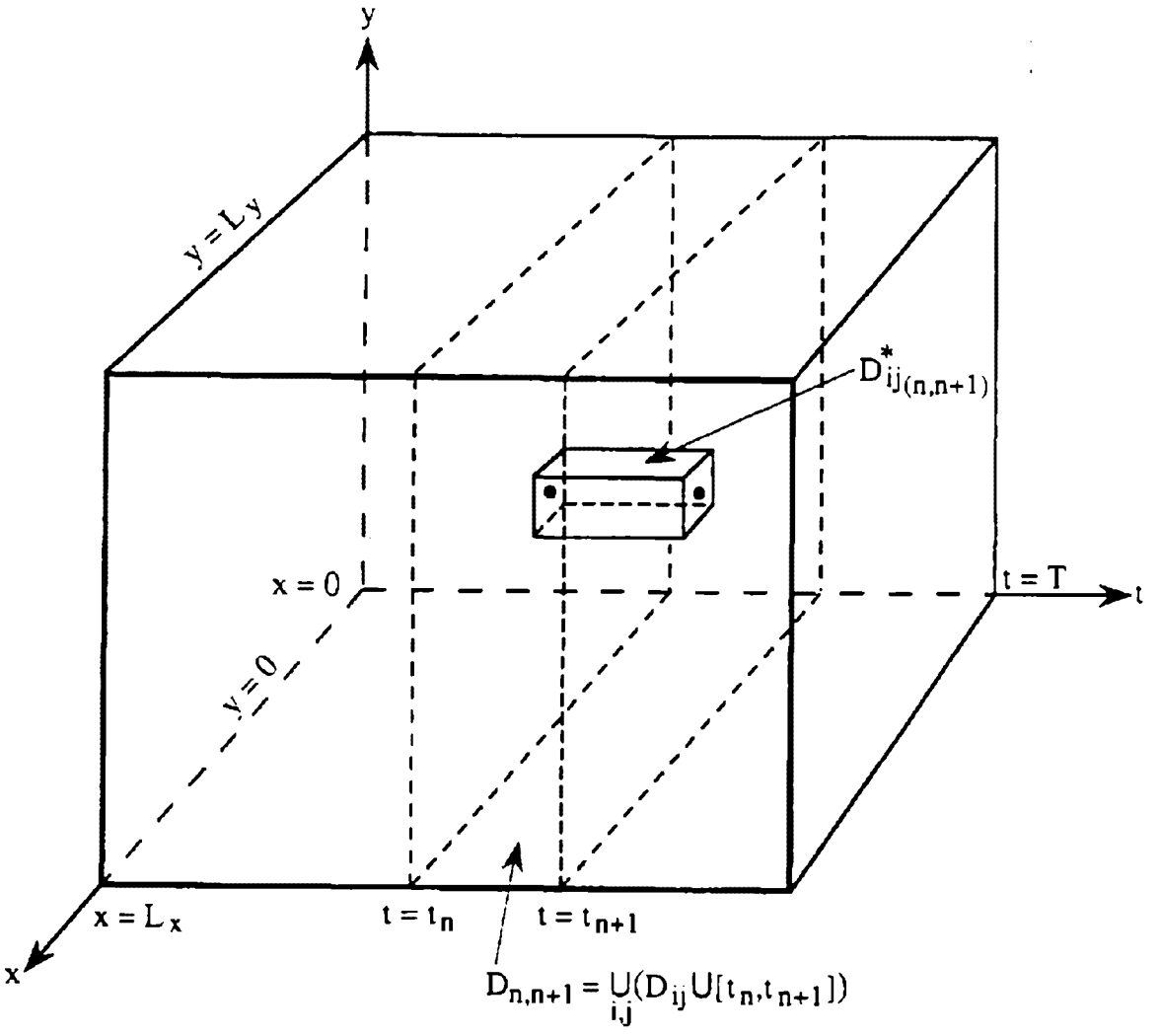

Figure 6. Relations of the subregions of the overall space-time cylinder to each other and the superimposed set of lattice points.

Lindstrom and Boersma (1990) give the necessary details of the approximation procedure where the nodal points are chosen in the mesh rather than in the center of each block. Now assume that the four compounds do not alter the flow field and that they may be treated independently of one another. Thus, using the previously developed equations, the generic equation approximating the transport and fate of each compound can be written as

$$\tilde{C}^*_{i,j,n+1} - \tilde{C}^*(P^*_{ij(n)}) + \frac{\Lambda^*_{ij}\ \Delta t}{1 + R^*_{ij}}\tilde{C}^*_{i,j,n} + \frac{\Delta t}{1 + R^*_{ij}}\lambda^*(x_i, y_j, t_n)$$

$$= a\ell t1^*_{ij}\ \tilde{C}^*_{i-1,j-1,n} + a\ell t2^*_{ij}\ \tilde{C}^*_{i-1,j,n} + a\ell t3^*_{ij}\ \tilde{C}^*_{i-1,j+1,n}$$

$$+ adt1^*_{ij}\ \tilde{C}^*_{i,j-1,n} + adt2^*_{ij}\ \tilde{C}^*_{i,j,n} + adt3^*_{ij}\ \tilde{C}^*_{i,j+1,n}$$

$$+ aut1^*_{ij}\ \tilde{C}^*_{i+1,j-1,n} + aut2^*_{ij}\ \tilde{C}^*_{i+1,j,n} + aut3^*_{ij}\ \tilde{C}^*_{i+1,j+1,n}$$

$$+ \frac{\Delta t}{\epsilon_{ij}(1 + R^*_{ij})}\left\{Q^*_{so_{ij}} + Q_{inj_{ij}}\left[C^*_{sour_{ij}} - \frac{\tilde{C}^*_{i,j,n}}{\rho_w}\right]\right\}, \qquad (5.3.4)$$

where the nine coefficients $a\ell t1^*_{i,j}$ $a\ell t2^*_{i,j}$, etc. are defined as follows:

$$a\ell t1^*_{ij} = \qquad (5.3.5)$$

$$\Delta t\left\{\frac{(\epsilon\ D^*_{xyi-1/2,j} + \epsilon\ D^*_{xyi,j-1/2})/4}{\{(\Delta x_{i-1} + \Delta x_i)/2\}\ \{(\Delta y_{j-1} + \Delta y_j)/2\}}\right\} / [\epsilon_{ij}(1 + R^*_{ij})]^{-1},$$

$$a\ell t2^*_{ij} = \qquad (5.3.6)$$

$$\Delta t\left\{\frac{\left(\frac{\Delta y_{j-1} + \Delta y_j}{2}\right)\frac{\epsilon D^*_{xxi-1/2,j}}{\Delta x_{i-1}} + \frac{(\epsilon D^*_{xyi,j-1/2} - \epsilon D^*_{xyi,j+1/2})}{4}}{\left\{\frac{(\Delta x_{i-1} + \Delta x_i)}{2}\right\}\left\{\frac{(\Delta y_{j-1} + \Delta y_j)}{2}\right\}}\right\} / [\epsilon_{ij}(1+R^*_{ij})],$$

$$a\ell t3^*_{ij} = \qquad (5.3.7)$$

$$-\Delta t\left\{\frac{\frac{(\epsilon\ D^*_{xyi,j+1/2} + \epsilon\ D^*_{xyi-1/2,j})}{4}}{\left\{\frac{(\Delta x_{i-1} + \Delta x_i)}{2}\right\}\left\{\frac{(\Delta y_{j-1} + \Delta y_j)}{2}\right\}}\right\} / [\epsilon_{ij}(1 + R^*_{ij})],$$

$$adt1^*_{ij} = \tag{5.3.8}$$

$$\Delta t\left\{\frac{\left(\frac{\Delta x_{i-1}+\Delta x_i}{2}\right)\frac{\epsilon D^*_{yyi,j-1/2}}{\Delta y_{j-1}}+\frac{(\epsilon D^*_{xyi-1/2,j}-\epsilon D^*_{xyi+1/2,j})}{4}}{\left\{\frac{(\Delta x_{i-1}+\Delta x_i)}{2}\right\}\left\{\frac{(\Delta y_{j-1}+\Delta y_j)}{2}\right\}}\right\}/[\epsilon_{ij}(1+R^*_{ij})],$$

$$adt2^*_{ij} = \tag{5.3.9}$$

$$-\Delta t\left\{\frac{\left(\frac{\Delta y_{j-1}+\Delta y_j}{2}\right)\left(\frac{\epsilon D^*_{xxi+1/2,j}}{\Delta x_i}+\frac{\epsilon D^*_{xxi-1/2,j}}{\Delta x_{i-1}}\right)}{\left\{\frac{(\Delta x_{i-1}+\Delta x_i)}{2}\right\}\left\{\frac{(\Delta y_{j-1}+\Delta y_j)}{2}\right\}}\right.$$

$$\left.+\frac{\left(\frac{\Delta x_{i-1}+\Delta x_i}{2}\right)\left(\frac{\epsilon D^*_{yyi,j+1/2}}{\Delta y_j}+\frac{\epsilon D^*_{yyi,j-1/2}}{\Delta y_{j-1}}\right)}{\left\{\frac{(\Delta x_{i-1}+\Delta x_i)}{2}\right\}\left\{\frac{(\Delta y_{j-1}+\Delta y_j)}{2}\right\}}\right\}/[\epsilon_{ij}(1+R^*_{ij})] ,$$

$$adt3^*_{ij} = \tag{5.3.10}$$

$$\Delta t\left\{\frac{\left(\frac{\Delta x_{i-1}+\Delta x_i}{2}\right)\frac{\epsilon D^*_{yyi,j+1/2}}{\Delta y_j}+\frac{(\epsilon D^*_{xyi+1/2,j}-\epsilon D^*_{xyi-1/2,j})}{4}}{\left\{\frac{(\Delta x_{i-1}+\Delta x_i)}{2}\right\}\left\{\frac{(\Delta y_{j-1}+\Delta y_j)}{2}\right\}}\right\}/[\epsilon_{ij}(1+R^*_{ij})],$$

$$aut1^*_{ij} = \tag{5.3.11}$$

$$-\Delta t\left\{\frac{\frac{(\epsilon D^*_{xyi+1/2,j}+\epsilon D^*_{xyi,j-1/2})}{4}}{\left\{\frac{(\Delta x_{i-1}+\Delta x_i)}{2}\right\}\left\{\frac{(\Delta y_{j-1}+\Delta y_j)}{2}\right\}}\right\}/[\epsilon_{ij}(1+R^*_{ij})] ,$$

$$aut2^*_{ij} = \tag{5.3.12}$$

$$\Delta t\left\{\frac{\left(\frac{\Delta y_{j-1} + \Delta y_j}{2}\right)\frac{\epsilon D^*_{xxi+1/2,j}}{\Delta x_i} + \frac{(\epsilon D^*_{xyi,j+1/2} - \epsilon D^*_{xyi,j-1/2})}{4}}{\left\{\frac{(\Delta x_{i-1} + \Delta x_i)}{2}\right\}\left\{\frac{(\Delta y_{j-1} + \Delta y_j)}{2}\right\}}\right\}/[\epsilon_{ij}(1+R^*_{ij})],$$

$$aut3^*_{ij} = \tag{5.3.13}$$

$$\Delta t\left\{\frac{\frac{(\epsilon\ D^*_{xyi+1/2,j} + \epsilon\ D^*_{xyi,j+1/2})}{4}}{\left\{\frac{(\Delta x_{i-1} + \Delta x_i)}{2}\right\}\left\{\frac{(\Delta y_{j-1} + \Delta y_j)}{2}\right\}}\right\}/[\epsilon_{ij}(1 + R^*_{ij})] \ .$$

$P^*_{ij(n)}$ is one of four points within D_{ij}, which is viewed as the position, at time t_n of that particle of compound * which lies on the trajectory or fluid flow path, passing through (x_i, y_j) at time t_{n+1}. A detailed explanation of how the node $P^*_{ij(n)}$ is found is given in Appendix A. With a good estimate of $P^*_{ij(n)}$ now available $C^*(P^*_{ij,n})$ is estimated, using the interpolation formulas given in Appendix A.

The mid-nodal point estimates of the various transverse, cross-axis, and longitudinal dispersion coefficients are defined to be

$$\epsilon\ D^*_{xxi+1/2,j} \doteq \frac{\epsilon\ D^*_{xxi+1,j} + \epsilon\ D^*_{xxi,j}}{2}\ , \tag{5.3.14}$$

$$\epsilon\ D^*_{xxi-1/2,j} \doteq \frac{\epsilon\ D^*_{xxi,j} + \epsilon\ D^*_{xxi-1,j}}{2}\ , \tag{5.3.15}$$

$$\epsilon\ D^*_{xyi+1/2,j} \doteq \frac{\epsilon\ D^*_{xyi+1,j} + \epsilon\ D^*_{xyi,j}}{2}\ , \tag{5.3.16}$$

$$\epsilon\ D^*_{xyi-1/2,j} \doteq \frac{\epsilon\ D^*_{xyi,j} + \epsilon\ D^*_{xyi-1,j}}{2}\ , \tag{5.3.17}$$

$$\epsilon D^*_{yxi,j+1/2} = \epsilon D^*_{xyi,j+1/2} \doteq \frac{\epsilon D^*_{xyi,j+1} + \epsilon D^*_{xyi,j}}{2} , \qquad (5.3.18)$$

$$\epsilon D^*_{yxi,j-1/2} = \epsilon D^*_{xyi,j-1/2} \doteq \frac{\epsilon D^*_{xyi,j} + \epsilon D^*_{xyi,j-1}}{2} , \qquad (5.3.19)$$

$$\epsilon D^*_{yyi,j+1/2} \doteq \frac{\epsilon D^*_{yyi,j+1} + \epsilon D^*_{yyi,j}}{2} , \qquad (5.3.20)$$

$$\epsilon D^*_{yyi,j-1/2} \doteq \frac{\epsilon D^*_{yyi,j} + \epsilon D^*_{yyi,j-1}}{2} . \qquad (5.3.21)$$

5.4. Boundary Conditions for Approximate Concentration Field

To complete the description of the approximate chemical concentration fields, $C^*_{i,j,n}$, the initial and boundary data must be specified.

5.4.1. Initial data

At time t = 0 days

$$\tilde{C}^*_{i,j,o} = C^*(x_i, y_j, 0^+) , \qquad (5.4.1)$$

completely specifies the initial data. Recalling the geometric interpretation of $C^*_{i,j,o}$, this means that over each region D_{ij} at time t = 0, the discrete approximation begins with the concentration of each chemical being constant in the space-time cylinder, with the value of the true concentration distribution * evaluated at nodal point (x_i, y_j).

5.4.2. Inlet and outlet end data

Recalling the definition of the inlet boundary concentration, $C^*_{in}(t)$, given by equation (5.2.5), define the constants

$$U_{in1} = \frac{1}{L_x} \int_0^{L_x} (\epsilon\ U_y)_{y=0} dx \ , \tag{5.4.2}$$

$$U^*_{in2} = \frac{1}{L_x} \int_0^{L_x} (\epsilon\ \frac{D^*_{yy}}{\Delta y_1} + \epsilon\ U_y)_{y=0} dx \ , \tag{5.4.3}$$

and function

$$U^*_{in3}(t) = \frac{1}{L_x} \int_0^{L_x} (\epsilon\ \frac{D^*_{yy}}{\Delta y_1})_{y=0}\ C^*\ (x, \Delta y_1, t) dx \ , \tag{5.4.4}$$

so that the differential equation defining $C^*_{in}(t)$ becomes

$$\frac{dC^*_{in}}{dt} = C^*_o \frac{U_{in1}}{L_{in}} + \frac{U^*_{in3}(t)}{L_{in}} - \frac{U^*_{in2}}{L_{in}} C^*_{in} \ . \tag{5.4.5}$$

This linear, first order, Bernoulli class ordinary differential equation can be shown to have the unique time convolution solution between the two time levels t_n and t_{n+1},

$$\exp[U^*_{in2}\ t_{n+1}/L_{in}]^* C_{in}\ (t_{n+1}) - \exp[U^*_{in2}\ t_n/\ L_{in}]^* C_{in}\ (t_n)$$

$$= \int_{t_n}^{t_{n+1}} (C^*_o \frac{U_{in1}}{L_{in}} + \frac{U^*_{in3}(t)}{L_{in}}) \exp\left[\frac{U^*_{in2}\ t}{L_{in}}\right] dt \ . \tag{5.4.6}$$

Assume that over $[t_n, t_{n+1}]$, $U^*_{in3}(t)$ is continuous and one-signed, and $\exp[U^*_{in2}t/L_{in}]$ is continuous and differentiable. This yields, upon multiplication of both sides by the expression $\exp[-U^*_{in2}t/L_{in}]$, the formula

$$C^*_{in}\ (t_{n+1}) = \exp[-U^*_{in2}\ \Delta t/L_{in}]^* C_{in}\ (t_n)$$

$$+ \frac{[C^*_o\ U_{in1} + U^*_{in3}\ (\zeta^*_n\ )]}{U^*_{in2}} \left[1 - \exp[-U^*_{in2}\ \Delta t/L_{in}]\right] \ , \tag{5.4.7}$$

where ζ^*_n is some value of time t in $[t_n, t_{n+1}]$. Since ζ_n is not known, its value is approximated by setting $\zeta^*_n = t_n$, thereby making equation (5.4.7) an explicit formula, which is in line with the explicit computing formula for the approximate free phase chemical concentration distribution, given by equation (5.3.4). The formula actually encoded is then based upon the recursive scheme

$$\chi^*_{in(n+1)} = \exp[-U_{in2}\ \Delta t/L_{in}]\ \chi^*_{in(n)}$$

$$+ \frac{[C_o\ U_{in1} + U^*_{in3}\ (t_n)]}{U_{in2}} (1 - \exp[-U^*_{in2}\ \Delta t/L_{in}]) , \qquad (5.4.8)$$

where $\chi_{in(n)}$ is the approximation to C^*_{in} at time t_n. The initial condition required to get this recursive scheme going is $\chi^*_{in(0)} = C^*_{in}(0)$ where the zero argument of C_{in} stands for the zero point in time.

Since $U_y(x,0)$ is not known, except at each nodal point, each of the three integrals stated by equations (5.4.2) through (5.4.4) is approximated by the trapezoidal rule as follows:

$$\int_0^{L_x} (\epsilon\ U_y)_{y=0} dx \doteq \sum_{k=1}^{N_x-1} I^{in}_{1k} , \qquad (5.4.9)$$

where

$$I^{in}_{1K} = \frac{\Delta x_k}{2} [\epsilon\ U_y(x_k,0) + \epsilon\ U_y(x_{k+1},0)], \qquad (5.4.10)$$

and

$$\int_0^{L_x} (\epsilon \frac{D^*_{yy}}{\Delta y_1} + \epsilon\ U_y)_{y=0} dx \doteq \sum_{k=1}^{N_x-1} I^{in}_{2k} , \qquad (5.4.11)$$

where

$$I_{2k}^{in} = \frac{\Delta x_k}{2} \left[\left(\frac{\epsilon\ D_{yy}^*}{\Delta y_1} + \epsilon\ U_y\right)_{(x_k,0)} + \left(\frac{\epsilon\ D_{yy}^*}{\Delta y_1} + \epsilon\ U_y\right)_{(x_{k+1},0)} \right], \qquad (5.4.12)$$

and

$$\int_0^{L_x} \left(\frac{\epsilon\ D_{yy}^*}{\Delta y_1}\right)_{y=0} C(x,\Delta y_1,t)dx \doteq \sum_{k=1}^{N_x-1} I_{3k}^{in}\ , \qquad (5.4.13)$$

where

$$I_{3k}^{in} = \frac{\Delta x_k}{2} \left[\left.\frac{\epsilon\ D_{yy}^*}{\Delta y_1}\right|_{(x_k,0)} C^*(x_k,\Delta y_1,t) + \left.\frac{\epsilon\ D_{yy}^*}{\Delta y_1}\right|_{(x_{k+1},0)} C^*(x_{k+1},\Delta y_1,t) \right] . \qquad (5.4.147)$$

U^*_{in1} and U^*_{in2} are calculated only once in time, but U^*_{in3} must be recalculated at every time step.

For the outlet tank and/or boundary condition, use equation (5.2.6) to define the constant

$$U_{out_1}^* = \frac{1}{L_x} \int_0^{L_x} \left(\left.\frac{\epsilon\ D_{yy}^*}{\Delta y_{Ny}}\right|_{y=L_y} + (\epsilon\ U_y) \right)_{y=L_y} dx \qquad (5.4.15)$$

and the function

$$U_{out_2}^*(t) = \frac{1}{L_x} \int_0^{L_x} \left(\left.\frac{\epsilon\ D_{yy}^*}{\Delta y_{Ny}}\right|_{y=L_y} + (\epsilon\ U_y) \right)_{y=L_y} C^*(x,L_y-\Delta y_{Ny},t)dx, \qquad (5.4.16)$$

so that the differential equation defining $C_{out}^*(t)$ becomes

$$\frac{dC_{out}^*}{dt} = -\frac{U_{out1}^*}{L_{out}} C_{out} + \frac{U_{out2}^*(t)}{L_{out}} . \qquad (5.4.17)$$

This first order Bernoulli ordinary differential equation (ODE) can be treated in the same way as the ODE for the inlet tank. Over the two time level interval $[t_n, t_{n+1}]$

$$\exp[U^*_{out1}\ t_{n+1}/L_{out}]\ C^*_{out}(t_{n+1}) - \exp[U^*_{out1}\ t_n/L_{out}]C^*_{out}(t_n)$$

$$= \int_{t_n}^{t_{n+1}} \frac{U^*_{out2}(t)}{L_{out}} \exp[U^*_{out1}\ t/L_{out}]\ dt\ . \tag{5.4.18}$$

Applying the mean value theorem again obtains, upon subsequently multiplying through both sides by $\exp[-U^*_{out1}/L_{out})t_{n+1}]$,

$$C^*_{out}(t_{n+1}) = \exp[-U^*_{out1}\ \Delta t/L_{out}]\ C^*_{out}(t_n)$$

$$+ \frac{U^*_{out2}(\eta^*_n)}{U_{out1}} (1 - \exp[-U_{out1}\ \Delta t/L_{out}])\ , \tag{5.4.19}$$

where η_n^* is a time point in the interval $[t_n, t_{n-1}]$. As before, $\eta_n^* = t_n$, is chosen to generate an explicit formula, approximating $C^*_{out}(t_{n-1})$, by $\chi^*_{out(n+1)}$ so that

$$\chi^*_{out(n+1)} = \exp[-U^*_{out1}\ \Delta t/L_{out}]\ \chi^*_{out(n)}$$

$$+ \frac{U^*_{out2}(t_n)}{U^*_{out1}} (1 - \exp[-U^*_{out1}\ \Delta t/L_{out}])\ . \tag{5.4.20}$$

Initially, set $\chi^*_{out(0)} = C^*_{out}(0)$, and apply equation (5.4.20) recursively, in conjunction with the evaluation of $U^*_{out2}(t_n)$.

As was done in the case of the inlet boundary, approximate

$$\int_0^{L_x} \left[\frac{\epsilon\ D^*_{yy}}{\Delta y_{Ny}} + (\epsilon\ U_y)\right]_{y=L_y} dx \doteq \sum_{k=1}^{N_x-1} I^{out}_{1k}\ , \tag{5.4.21}$$

where

$$I_{1k}^{out} = \frac{\Delta x_k}{2} \left\{ \left[\frac{\epsilon\ D_{yy}^*}{\Delta y_{Ny}} + (\epsilon U_y) \right] \Bigg|_{(x_k, L_y)} + \left[\frac{\epsilon\ D_{yy}^*}{\Delta y_{Ny}} + (\epsilon U_y) \right] \Bigg|_{(x_{k+1}, L_y)} \right\} \quad (5.4.22)$$

and

$$\int_0^{L_x} \left[\frac{\epsilon\ D_{yy}^*}{\Delta y_{Ny}} + (\epsilon\ U_y) \right] \Bigg|_{y=L_y} C^*(x, L_y - \Delta y_{Ny}, t) dx \doteq \sum_{k=1}^{N_x - 1} I_{2k}^{out}(t) \quad (5.4.23)$$

where

$$I_{2k}^{out}(t) = \frac{\Delta x_k}{2} \left\{ \left[\frac{\epsilon\ D_{yy}^*}{\Delta y_{Ny}} + (\epsilon\ U_y) \right] \Bigg|_{(x_k, L_y)} C^*(x_k, L_y - \Delta y_{Ny}, t) \right.$$

$$\left. + \left[\frac{\epsilon\ D_{yy}^*}{\Delta y_{Ny}} + (\epsilon\ U_y) \right] \Bigg|_{(x_{k+1}, L_y)} C^*(x_{k+1}, L_y - \Delta y_{Ny}, t) \right\} . \quad (5.4.24)$$

While U^*_{out1} is a constant and calculated *a priori* with respect to time, U^*_{out2} is time dependent and must be recalculated at each time step.

5.4.3. Zero flux walls

The conditions of zero chemical flux boundaries at $x = 0$ and $x = L_x$ follow from equations (4.3.5) and (4.3.6):

$$\tilde{C}^*_{0,j,n} = \frac{\left[2 + \frac{\Delta x_2}{\Delta x_1} + \frac{\Delta x_1}{\Delta x_2} \right] \tilde{C}^*_{1,j,n} - \frac{\Delta x_1}{\Delta x_2} \tilde{C}^*_{2,j,n}}{2 + \frac{\Delta x_2}{\Delta x_1}} \quad (5.4.25)$$

and

$$\bar{C}^*_{Nx,j,n} = \frac{-\dfrac{\Delta x_{Nx}}{\Delta x_{Nx-1}}\,\bar{C}^*_{Nx-2,j,n} + \left(2 + \dfrac{\Delta x_{Nx}}{\Delta x_{Nx-1}} + \dfrac{\Delta x_{Nx-1}}{\Delta x_{Nx}}\right)\bar{C}^*_{Nx-1,j,n}}{2 + \dfrac{\Delta x_{Nx-1}}{\Delta x_{Nx}}} \qquad (5.4.26)$$

for $j = 1,2,\ldots N_{y-1}$.

5.5. Approximate Microbial Populations

The microbial populations at each point in space and time satisfy the first order process laws stated by equations (5.1.11) and (5.1.12)

$$\frac{\partial N_1}{\partial t}(x,y,t) = \omega_1(x,y,t)N_1 \qquad (\text{kg kg}^{-1}\ \text{day}^{-1}) \qquad (5.5.1)$$

and

$$\frac{\partial N_2}{\partial t}(x,y,t) = \omega_2(x,y,t)N_2 \qquad (\text{kg kg}^{-1}\ \text{day}^{-1}) \qquad (5.5.2)$$

where the two first order rate coefficient functions are defined by

$$\omega_1 = Y^1_{so}\ r^1_{sonu} - \delta^1 + Y^1_{sni}\ r^1_{sninu} \qquad (5.5.3)$$

and

$$\omega_2 = Y^2_{so}\ r^2_{sonu} - \delta^2\ . \qquad (5.5.4)$$

Assuming that at time $t = 0$ days, $N_1(x,y,0)$ and $N_2(x,y,0)$ are both known initial distributions, the formulas

$$N_1(x,y,t_{n+1}) = N_1(x,y,t_n)\ \exp\left[\int_{t_n}^{t_{n+1}} \omega_1(x,y,\tau)d\tau\right] \qquad (5.5.5)$$

and

$$N_2(x,y,t_{n+1}) = N_2(x,y,t_n) \exp[\int_{t_n}^{t_{n+1}} \omega_2(x,y,\tau)d\tau] \tag{5.5.6}$$

are easily obtained. Application of the mean value theorem to the integrals in equations (5.5.5) and (5.5.6) yields

$$N_1(x,y,t_{n+1}) = N_1(x,y,t_n) \exp[\Delta t\ \omega_1(x,y,\tau_{1n})] \tag{5.5.7}$$

and

$$N_2(x,y,t_{n+1}) = N_2(x,y,t_n) \exp[\Delta t\ \omega_2(x,y,\tau_{2n})] \ , \tag{5.5.8}$$

where both τ_{1n} and τ_{2n} are values of time t in $[t_n, t_{n+1}]$. Up to this point no approximations have been made in the development of the representations of the two microbial populations over time. By choosing both τ_{1n} and τ_{2n} equal to t_n, the approximating populations are defined recursively to be

$$\tilde{N}_1(x,y,t_{n+1}) = \tilde{N}_1(x,y,t_n) \exp[\Delta t\ \omega_1(x,y,t_n)] \tag{5.5.9}$$

and

$$\tilde{N}_2(x,y,t_{n+1}) = \tilde{N}_2(x,y,t_n) \exp[\Delta t\ \omega_2(x,y,t_n)] \ . \tag{5.5.10}$$

It is clear from the definitions of ω_1 and ω_2 and the mathematical structure of formulas (5.5.9) and (5.5.10) that whenever ω_1 and ω_2 are greater than zero the two populations are increasing and unstable. Whenever ω_1 and ω_2 are equal to zero, the populations are constant, i.e. stable at their respective values whenever ω_1 and ω_2 were first zero. If ω_1 and ω_2 are less than zero the populations are decreasing (stable) and will eventually cease to exist. Equations (5.5.9) and (5.5.10) are used in the model LT3VSI.

5.6. Stability Considerations

Since the computing scheme defined by equation (5.3.4) is explicit, a stability criterion arises. Richtmyer and Morton (1967), Varga (1962), and Reddell and Sunada (1970) have established that by choosing

$$\Delta t_0^* \le \frac{0.5}{\max\limits_{i,j}\left(\frac{D^*_{xxij}}{\Delta x_i^2} + \frac{D^*_{yyij}}{\Delta x_j^2}\right)} \tag{5.6.1}$$

the computing scheme will be stable when the local Courant numbers are less than or equal to 1.0 and there are no losses or chemical injections present. However, Cheng et al. (1984) claim that a sufficient condition for stability is

$$\Delta t_1^* \le \frac{1}{\max\limits_{i,j}\left\{\frac{|U^*_{xij}|}{\Delta x_i} + \frac{|U^*_{yij}|}{\Delta y_i} + 2\left(\frac{D^*_{xxij}}{\Delta x_i^2} + \frac{D^*_{yyij}}{\Delta y_j^2}\right)\right\}} , \tag{5.6.2}$$

which is a tighter restriction than that given by equation (5.6.1). Because the flow field is at steady state, it is a simple matter to calculate this value of Δt before the start of the chemical transport and fate computation. The Δt value, obtained initially so that the local Courant numbers are less than or equal to 1, is defined by

$$\Delta t_2^* \le \min\limits_{i,j}\left\{\frac{\Delta x_{i-1}}{2|U_x^*|} , \frac{\Delta y_{j-1}}{2|U_y^*|}\right\} . \tag{5.6.3}$$

This condition guarantees that the stream line and the particle of interest "riding" on that stream line, going through (x_i, y_i) at time t_{n+1} must also pass through $P^*_{ij(n)}$ at time t_n. The addition of distributed first order losses and the presence of injection wells further

reduce the magnitude of Δt. These important restrictive conditions will be satisfied by choosing Δt so that

$$\Delta t_3^* \leq \tag{5.6.4}$$

$$\left[\max_{ij}\left\{\frac{\Lambda^*}{1+R_{ij}^*} + \frac{Q_{inj_{ij}}}{\epsilon(1+R_{ij}^*)\rho_w} + \frac{2|U_{xij}^*|}{\Delta x_i} + \frac{2|U_{yij}^*|}{\Delta y_j} + 2\left(\frac{D_{xxij}^*}{\Delta x_i^2} + \frac{D_{yyij}^*}{\Delta y_j^2}\right)\right\}\right]^{-1}$$

The presence of the complex rates for utilization of chemical compounds by microbes rules also affects the choice of the maximum allowable time step size. Careful inspection of equations (5.1.21) through (5.1.24), which define the loss rate functions, and equations (5.1.8) through (5.1.10), which define the utilization rates, clearly shows that the chemical concentration C^* appears linearly in the numerator of each loss function, λ^*. Since each C^* is nonnegative it is easy to define a set of positive upper bounds upon λ^*, one for each compound $*$, which depends linearly upon C^*. For example, the bound on λ^{nu}

$$0 \leq \lambda^{nu} \leq B^{nu}(N_1, N_2)C^{nu} \tag{5.6.5}$$

where

$$B^{nu}(N_1, N_2) = \frac{\rho_b}{\epsilon}\left\{\left(\psi_o^1 \frac{\mu_o^1}{Y_{so}^1}\frac{1}{K_{onu}^1} + \theta_{ni}^1 \frac{\mu_{ni}^1}{Y_{sni}^1}\frac{1}{K_{ninu}^1}\right) N_1 + \psi_o^2 \frac{\mu_o^2}{Y_{so}^2}\frac{1}{K_{onu}^2} N_2\right\} \tag{5.6.6}$$

The other three bounds have similar forms. For stability purposes then define that

$$\Delta t_4^* =$$

$$\left[\max_{ij}\left\{\frac{\Lambda^*}{1 + R_{ij}^*} + \frac{B^*(N_1,N_2)}{1 + R_{ij}^*} + \frac{Q_{inj_{ij}}}{\epsilon\ \rho_w(1 + R_{ij}^*)} + \frac{2|U_{xij}^*|}{\Delta x_i} + \frac{2|U_{yij}^*|}{\Delta y_j}\right.\right.$$

$$\left.\left. + 2\left(\frac{D_{xxij}^*}{\Delta x_i^2} + \frac{{}^*D_{yyij}}{\Delta y_j^2}\right)\right\}\right]^{-1} \qquad (5.6.7)$$

Since B^* is a function of the mass of the microbial population per unit mass of aquifer material which changes with time, we must be very careful to recompute Δt_4^*, periodically. A rule for periodically checking on the magnitudes of the B^* values is included in the Fortran 77 code, LT3VSI.

We then choose

$$\Delta t \le \min_* \{\Delta t_4^*\} \qquad (5.6.8)$$

which will be used as the sufficient stability criterion.

6. CONCLUSIONS FOR THE MODEL

Methods were developed for solving equations that describe transport and fate of chemicals in laboratory scale models of aquifers. The mathematical model is for aquifers consisting of a single layer of material, which can be either heterogeneous or homogeneous and anisotropic or isotropic with respect to the water flow field and heterogeneous or homogeneous but isotropic with respect to the chemical transport field properties.

The two-dimensional transport and fate model can be used for study of the important aspects of bioremediation of aquifers contaminated with

nitrogen. A broad range of aquifer remediation scenarios may be considered. These scenarios could include studies of placement of injection/extraction wells to induce plume spreading or plume shaping and the effects of regions of varying hydraulic conductivity on the shape of the plumes. The comprehensive treatment of the inlet and exit port induced boundary conditions, included with the analysis represents a significant step forward in modeling the transport and fate of chemicals in laboratory scale physical aquifers.

7. LITERATURE CITED

Bachelor, G. A., D. E. Cawlfield, F. T Lindstrom and L. Boersma. 1990. Denitrification in nonhomogeneous laboratory scale aquifers: 2. User's manual for the preliminary mathematical model LT2VSI. Special Report No. 865, Agric. Exp. Sta., Oregon State University, Corvallis, OR. 158 pp.

Baptista, A. M. de M. 1986. Accuracy analysis of the backward method of characteristics. In: VI. Intnl. Conf. on Finite Elements in Water Resources, Lisbon, Portugal, June 1986.

Baptista, A. M. de M. 1987. Solution of advection dominated transport by Eulerian-Lagrangian methods using the backward method of characteristics. Ph.D. Thesis. Dept. of Civil Eng., MIT, Cambridge, MA. 260 pp.

Baptista, A. M. de M., E. E. Adams and K. D. Stolzenbach. 1984. Eularian-Lagrangian analysis of pollutant transport in shallow water. Ralph M. Parsons Lab Rept. #296, Dept. of Civil Eng., MIT, Cambridge, MA 02139.

Bear, J. and A. Verruijt. 1987. Modeling Groundwater Flow and Pollution. Reidel Pub. Co., Dordrecht. 414 pp.

Bloomfield, P. 1976. Fourier Analysis of Time Series: An Introduction. Wiley, New York. 258 pp.

Bodvarsson, G. 1984. Linearization techniques and surface operators in the theory of unconfined aquifers. Water Resour. Res. 20:1271-1276.

Boersma, L. and F. T. Lindstrom. 1990. Denitrification in nonhomogeneous laboratory scale aquifers: 3. Simulated application of the prelimninary model (in preparation).

Cheng, R. T., V. Casulli and S. N. Milford. 1984. Eulerian-Lagrangian solution of the convection-dispersion equation in natural coordinates. Water Resour. Res. 20:944-952.

Herbert, D. 1958. Some Principles of Continuous Culture. In: Recent Progress in Microbiology. Edited by G. Tunevall, Blackwell Scientific, Boston, MA.

Konikow, L. F. and J. D. Bredehoeft. 1978. Computer model of two-dimensional solute transport and dispersion in ground water. In: Techniques of Water-Resources Investigations of the United States Geological Survey, Book 7, Chapter C2.

Kreyszig, E. 1979. Advanced Engineering Mathematics, 4th Ed. Wiley, New York. 939 pp.

Lindstrom, F. T. and L. Boersma. 1990. Denitrification in nonhomogeneous laboratory scale aquifers: 1. Preliminary model for transport and fate of a single compound. USEPA RSKERL (in press).

Lindstrom, F. T., L. Boersma, M. A. Barlaz and F. Beck. 1989. Transport and fate of water and chemicals in laboratory scale, single layer, aquifers. Vol. 1: Mathematical model. Spec. Rept. No. 845, Agric. Exp. Sta., Oregon State University, Corvallis, OR. 52 pp.

Molz, F. J., M. A. Widdowson and L. D. Benefield. 1986. Simulation of microbial growth dynamics coupled to nutrient and oxygen transport in porous media. Water Resour. Res. 22:1207-1216.

Parker, J. C. and M. Th. Van Genuchten. 1984. Flux-averaged and volume-averaged concentrations in continuum approaches to solute transport. Water Resour. Res. 20:866-872.

Prenter, P. M. 1975. Splines and Variational Methods. Wiley, New York. 323 pp.

Reddell, D. L. and D. K. Sunada. 1970. Numerical simulation of dispersion in groundwater aquifers. Colorado State Univ. Hydrology Paper No. 41. 79 pp.

Richtmyer, R. D. and K. W. Morton. 1967. Difference Methods for Initial-Value Problems. Interscience Publishers, Inc., New York. 405 pp.

Stone, H. L. 1968. Iterative solution of implicit approximations of multidimensional partial differential equations. Soc. Ind. Appl. Math. J. on Num. Anal. 5:530-558.

Varga, R. S. 1962. Matrix Iterative Analysis. Prentice-Hall, Englewood Cliffs, NJ. 322 pp.

Vemuri, V. and W. J. Karplus. 1981. Digital Computer Treatment of Partial Differential Equations. Prentice-Hall, Englewood Cliffs, NJ. 449 pp.

Widdowson, M. A., F. J. Molz and L. D. Benefield. 1988. A numerical transport model for oxygen- and nitrate-based respiration linked to substrate and nutrient availability in porous media. Water Resour. Res. 24:1553-1565.

Yates, S. R. 1988a. An analytical solution to saturated flow in a finite stratified aquifer. Ground Water 26:199-206.

Yates, S. R. 1988b. Seepage in a saturated-stratified aquifer with recharge. Soil Sci. Soc. Am. J. 52:356-363.

APPENDIX A

The methods used to find the particle tracking point $P^*_{i,j,n}$ and to subsequently estimate the chemical concentration $C(P^*_{i,j,n})$ are described below. This presentation requires discussion of the double Fourier integral representation of a specialization of the generic transport and fate equation. The two-dimensional procedures used in this analysis are extensions of the one-dimensional procedures developed and discussed by Baptista et al. (1984), Baptista (1986), and Baptista (1987). Figure A.1 shows the subregion $Đ_{ij}$ enclosing the node (x_i, y_j) and the eight surrounding nodes with their positions defined. U_x^* and U_y^* are signed quantities and are once continuously differentiable functions of the space coordinates everywhere, except perhaps on top of the wells. The procedure for finding P^*_{ijn} is described first.

A.1 Locating point P^*_{ijn}

The selection rules for finding point P^*_{ijn} are defined as follows:

i) if $U_x^* \geq 0$, $U_y^* \geq 0$, $P^*_{ij(n)}$ lies in subregion I

ii) if $U_x^* < 0$, $U_y^* \geq 0$, $P^*_{ij(n)}$ lies in subregion II

iii) if $U_x^* \geq 0$, $U_y^* < 0$, $P^*_{ij(n)}$ lies in subregion III

iv) if $U^*_x < 0$, $U_y^* < 0$, $P^*_{ij(n)}$ lies in subregion IV

The details of the estimate for the position of $P*_{ij(n)}$ are described for subregion 1, but similar arguments apply to subregions II, III, and IV.

Since U_x^* and U_y^* have been computed at every nodal point in Đ, U_x^* and U_y^* are known at (x_i, y_j) and the eight surrounding nodal points (Figure A.1). Figure A.2 shows an enlargement of region I with flow lines

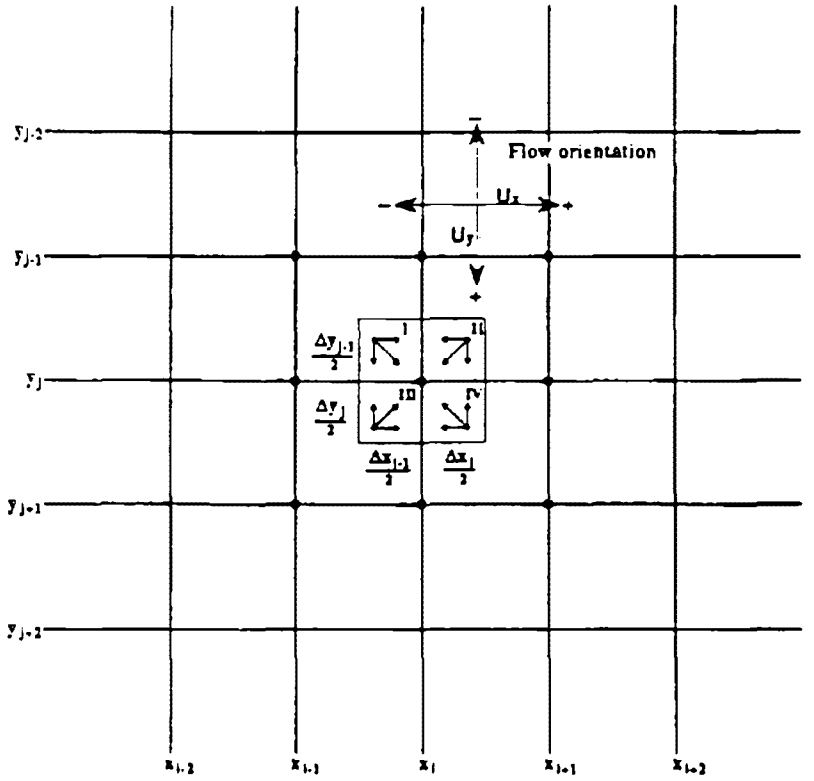

Figure A.1. Subregion D_{ij} divided into four separate subregions, one of which contains point $P^*_{ij(n)}$. Flow orientation is also shown.

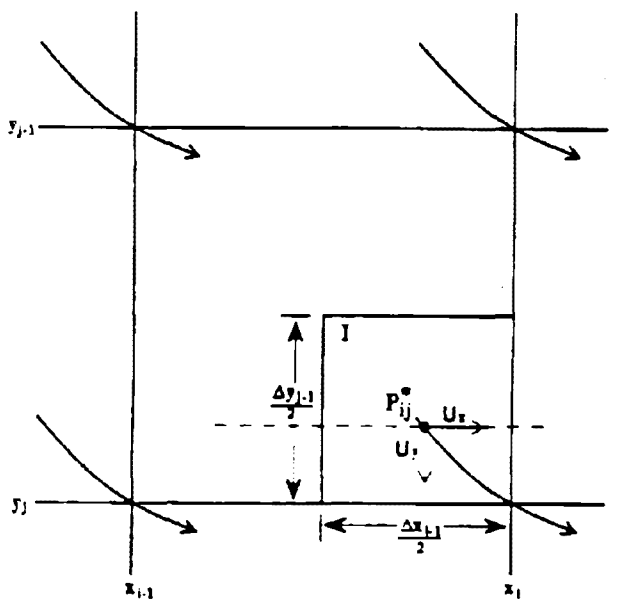

Figure A.2. Details of procedure used to find position of point $P^*_{ij(n)}$ in region I.

sketched in. The effective seepage velocity components U^*_x and U^*_y are approximated by the following bilinear interpolation formulas:

$$U^*_x = A^I_1 + B^I_1(x - x_i) + C^I_1(y - y_j) + D^I_1(x - x_i)(y - y_j) \ , \tag{A.1.1}$$

$$\tilde{U}^*_y = A^I_2 + B^I_2(x - x_i) + C^I_2(y - y_j) + D^I_2(x - x_i)(y - y_j) \ , \tag{A.1.2}$$

where the coefficients are defined by:

$$A^I_1 = U^*_{xi,j} \ , \qquad A^I_2 = U^*_{yi,j} \ , \tag{A.1.3}$$

$$B^I_1 = \frac{U^*_{xi,j} - U^*_{xi-1,j}}{\Delta x_{i-1}} \ , \qquad B^I_2 = \frac{U^*_{yi,j} - U^*_{yi-1,j}}{\Delta x_{i-1}} \ , \tag{A.1.4}$$

$$C^I_1 = \frac{U^*_{xi,j} - U^*_{xi,j-1}}{\Delta y_{j-1}} \ , \qquad C^I_2 = \frac{U^*_{yi,j} - U^*_{xi,j-1}}{\Delta y_{j-1}} \ , \tag{A.1.5}$$

$$D^I_1 = \frac{U^*_{xi,j} + U^*_{xi-1,j-1} - U^*_{xi-1,j} - U^*_{xi,j-1}}{\Delta x_{i-1}\ \Delta y_{j-1}} \ ,$$

$$D^I_2 = \frac{U^*_{yi,j} + U^*_{yi-1,j-1} - U^*_{yi-1,j} - U^*_{yi,j-1}}{\Delta x_{i-1}\ \Delta y_{j-1}} \ , \tag{A.1.6}$$

so that both $\tilde{U}_x^*$ and $\tilde{U}_y^*$ interpolate U_x^* and U_y^* exactly at the four corner points.

Since

$$\frac{dx}{dt} = U^*_x \quad \text{and} \quad \frac{dy}{dt} = U^*_y \ , \tag{A.1.7}$$

integrating both sides over $[t_n, t_{n+1}]$ yields

$$x(t_{n+1}) = x(t_n) + \int_{t_n}^{t_{n+1}} U^*_x \, dt \ , \tag{A.1.8}$$

$$y(t_{n+1}) = y(t_n) + \int_{t_n}^{t_{n+1}} U_y^* \, dt \ , \tag{A.1.9}$$

where now $[x(t_{n+1}), y(t_{n+1})] = (x_i, y_j)$ and $[x(t_n), y(t_n)] = P^*_{ij(n)} = [x^*_{i(n)}, y^*_{j(n)}]$. The relationships (A.1.6) and (A.1.7) are approximated in a manner analogous to the low order accuracy, time quadrature, approximation used in the main transport and fate equation (equation 5.3.4):

$$x_i = x_i^* + \Delta t \, \tilde{U}_x^* \tag{A.1.10}$$

and

$$y_i = y_i^* + \Delta t \, \tilde{U}_y^* \ . \tag{A.1.11}$$

Substituting for U_x^* and U_y^* leads to the coupled system of nonlinear algebraic equations in (x_i^*, y_j^*):

$$f_1^I(x_i^*, y_j^*) = x_i^* - x_i + \Delta t[A_1^I + B_1^I(x_i^* - x_i) + C_1^I(y_j^* - y_j) + D_1^I(x_i^* - x_i)(y_j^* - y_j)] = 0 \tag{A.1.12}$$

$$f_2^I(x_i^*, y_j^*) = y_j^* - y_j + \Delta t[A_2^I + B_2^I(x_i^* - x_i) + C_2^I(y_j^* - y_j) + D_2^I(x_i^* - x_i)(y_j^* - y_j)] = 0 \ . \tag{A.1.13}$$

The method of Newton-Raphson-Kantorovic (Vemuri and Karplus, 1981) is used to find (x_i^*, y_j^*), with (x_i, y_i) as the initial guess and a relative error tolerance of 10^{-4}. The theorem, which states that the nonlinear system of equations (A.1.12) and (A.1.13) has a unique solution inside subregion I, for the condition that A^I_1, A^I_2, B^I_1, B^I_2, C^I_1, C^I_2, D^I_1, and D^I_2 are all finite and that Δt is chosen so that

$$\Delta t \leq \min\left\{\frac{\Delta x_{i-1}}{2|U_x^*|}, \frac{\Delta y_{j-1}}{2|U_y^*|}\right\}, \tag{A.1.14}$$

can readily be proven. This proof is not shown here.

A.2 Fourier Component Analysis Under Special Hypothesis

Suppose that instead of working with a finite size domain Đ, we let the side walls and the inlet and outlet ports recede to infinity. This is an acceptable assumption for conditions where regions influenced by the injection/extraction wells and/or regions with initial distributions of compound are small relative to the longitudinal and transverse dimensions of the aquifer. For a homogeneous and isotropic aquifer with a velocity field that is constant in time and space, the generic transport equation (5.1.25) reduces to the form

$$\frac{dC^*}{dt} = \left\{D_{xx}^* \frac{\partial^2 C}{\partial x^2} + 2D_{xy}^* \frac{\partial^2 C}{\partial x \partial y} + D_{yy}^* \frac{\partial^2 C}{\partial y^2}\right\} / (1 + R^*)$$

$$+ \frac{Q_{so}^* + Q_{inj}\, C_{sour}^*}{\epsilon(1 + R^*)} \quad . \tag{A.2.1}$$

under the assumption that loss processes are not operating in the aquifer. Q^*_{so}, Q_{inj}, and Q_{out} may be considered to have a zero value everywhere in the space time cylinder $Đ^+$, where

$$Đ^+ = Đ \cup [0,T).$$

without loss of concept.

The next step is to define the double Fourier transform of some function f(x,y) which satisfies Dirichlet conditions (Kreyszig, 1979) to be

$$F(\zeta,\eta) = \int_{-\infty}^{+\infty}\int_{-\infty}^{+\infty} f(x,y)\ e^{-i(\zeta x+\eta y)}\ dxdy \tag{A.2.2}$$

where $i = \sqrt{-1}$, and to specifically assume that the initial distribution of chemical * is double Fourier transformable, i.e.

$$\hat{C}^*(\zeta,\eta,0) = \int_{-\infty}^{+\infty}\int_{-\infty}^{+\infty} C^*(x,y,0^+)\ e^{-i(\zeta x+\eta y)}\ dxdy \quad . \tag{A.2.3}$$

The double Fourier transformation of equation (A.2.1) obtains the form

$$\hat{C}^*(\zeta,\eta,t) = \hat{C}^*(\zeta,\eta,0^+)\ e^{-\frac{(\zeta^2 D^*_{xx}+2\zeta\eta D^*_{xy}+\eta^2 D^*_{yy})t}{1+R^*}}\ e^{-i\zeta V^*_x t}\ e^{-i\eta V^*_y t} \ . \tag{A.2.4}$$

Since the inversion double Fourier integral can be written as

$$f(x,y) = \frac{1}{4\pi^2}\int_{-\infty}^{+\infty}\int_{-\infty}^{+\infty} F(\zeta,\eta)\ e^{i(\zeta x+\eta y)}\ d\zeta d\eta \tag{A.2.5}$$

the solution to the sourceless form of equation (A.2.1) can be written as

$$C^*(x,y,t) = \frac{1}{4\pi^2}\int_{-\infty}^{+\infty}\int_{-\infty}^{+\infty} \hat{C}^*(\zeta,\eta,t)\ e^{i(\zeta x+\eta y)}\ d\zeta d\eta \quad . \tag{A.2.6}$$

Substitution of definition (A.2.4) into (A.2.6) yields the double Fourier integral (series) representation of the solution to the infinite 2-space Cauchy problem (A.2.1) as

$$C^*(x,y,t) = \frac{1}{4\pi^2}\int_{-\infty}^{+\infty}\int_{-\infty}^{+\infty} \hat{C}^*(\zeta,\eta,,0^+)\ e^{-\frac{(\zeta^2 D^*_{xx}+2\zeta\eta D^*_{xy}+\eta^2 D^*_{yy})t}{1+R^*}} \bullet$$

$$e^{i\zeta(x-V^*_x t)+i\eta(y-V^*_y t)}\ d\zeta d\eta \quad . \tag{A.2.7}$$

Equation (A.2.7) is the linear combination of a continuum of two dimensional right moving damped waves. The Fourier variables ζ and η have the dimensions of inverse wavelength and are referred to as the wave numbers in the x and y directions, respectively. The Fourier transform $F(\zeta,\eta)$ relates directly to the energy spectrum of the wave train $f(x,y)$ and is therefore referred to as the "power or energy spectrum" by the electrical engineers (Bloomfield, 1976). If D^*_{xx}, D^*_{xy}, and D^*_{yy} all equal zero, then equation (A.2.7) is the solution to the embedded two dimensional hyperbolic (wave) equation obtained by setting these same three dissipation parameters equal to zero in equation (A.2.1).

In the remainder we are interested in the double Fourier representation evaluated at an arbitrary grid point (x_ℓ, y_m) in $\mathcal{D}$. With time partitioned into discrete finite length subintervals of length Δt and with a uniform partitioning of the x-axis into subintervals of length Δx and the y-axis into subintervals of length Δy, we have

$$C^*(x_\ell, y_m, t_n) = \frac{1}{4\pi^2} \int_{-\infty}^{+\infty}\int_{-\infty}^{+\infty} \hat{C}^*(\zeta,\eta,0^+)\, e^{-\frac{(\zeta^2 D^*_{xx} + 2\zeta\eta D^*_{xy} + \eta^2 D^*_{yy})n\Delta t}{1 + R^*}} \cdot$$

$$e^{i\zeta(x_\ell - \frac{V^*_x \Delta t}{\Delta x} n\Delta x)}\, e^{i\eta(y_m - \frac{V^*_y \Delta t}{\Delta y} n\Delta y)}\, d\zeta\, d\eta$$

or:

$$C^*(x\ ,y\ ,t\ ) = \frac{1}{4\pi^2} \int_{-\infty}^{+\infty}\int_{-\infty}^{+\infty} \hat{C}^*(\zeta,\eta,0^+)\, R_E^n(\zeta,\eta)$$

$$e^{i(\zeta x_\ell + \eta y_m - n\Phi_E(\zeta,\eta)}\, d\zeta\, d\eta\ , \qquad \text{(A.2.8)}$$

where the amplitude per time step factor $R_E(\zeta,\eta)$ is defined by

$$R_E(\zeta,\eta,) = e^{-\left(\frac{(\zeta^2 D^*_{xx}+2\zeta\eta D^*_{xy}+\eta^2 D^*_{yy})n\Delta t}{1 + R^*}\right)}$$

and the total phase angle per time step $\Phi_E(\zeta,\eta)$ is defined by

$$\Phi_E(\zeta,\eta) = C_{rx}\zeta\Delta x + C_{ry}\eta\Delta y = \Phi_{Ex}(\zeta,\eta) + \Phi_{Ey}(\zeta,\eta) \qquad (A.2.10)$$

with C_{rx} being the x-coordinate Courant number

$$C_{rx} = \frac{V^*_x\Delta t}{\Delta x} \quad . \qquad (A.2.11)$$

and C_{ry} being the y-coordinate Courant number

$$C_{ry} = \frac{V^*_y\Delta t}{\Delta y} \quad . \qquad (A.2.12)$$

Quantities $\Phi_{Ex}/\zeta\Delta t$ and $\Phi_{Ey}/\eta\Delta t$ have dimensions of effective seepage velocity in the x and y direction, respectively. The reason for rearranging the exact solution into the form given by equation (A.2.8) is that much the same form is obtained for each numerical approximation method chosen (both finite difference and finite element), with the differences coming from the definitions of the amplitude per time step and the phase angle per time step. Distribution (A.2.8) is the standard or reference distribution when the amplitude and phase angles per time step are defined by the equations (A.2.9) and (A.2.10). The definition of the two Courant numbers are universal and hold for both the exact and approximate solutions.

Two alternative methods for estimating $C^*(P_{ijn})$ have been encoded in the numerical model LT3VSI. An in-depth Fourier analysis of the first

of these methods is now considered, using the above outlined specialized hypothesis.

A.3 Alternatives for Estimating $C^*(P_{ijn})$

A.3.1 Alternative 1: Bilinear Lagrange Polynomials

Since point P^*_{ijn} is rarely, if ever, a nodal point, $C^*(P_{ijn})$ must be estimated using an interpolation formula. The logical first choice for an interpolation formula is the bilinear Lagrange polynomial. This is shown by continuing with the assumption that P^*_{ijn} lies in subregion 1 in Figure A.1.

Approximate $C^*(P^*_{ijn})$ using the formula

$$\tilde{C}^*(P^*_{ijn}) = \frac{(x_i^* - x_i)(y_j^* - y_j)}{(x_{i-1} - x_i)(y_{j-1} - y_j)} \tilde{C}^*_{i-1,j-1,n}$$

$$+ \frac{(x_i^* - x_{i-1})(y_j^* - y_j)}{(x_i - x_{i-1})(y_{j-1} - y_j)} \tilde{C}^*_{i,j-1,n}$$

$$+ \frac{(x_i^* - x_i)(y_j^* - y_{j-1})}{(x_{i-1} - x_i)(y_j - y_{j-1})} \tilde{C}^*_{i-1,j,n}$$

$$+ \frac{(x_i^* - x_{i-1})(y_j^* - y_{j-1})}{(x_i - x_{i-1})(y_j - y_{j-1})} \tilde{C}^*_{i,j,n} \quad . \qquad \text{(A.3.1.1)}$$

Formula (A.3.1.1) has been obtained by applying the product basis assumption and the Lagrange canonical basis functions for the set of all piecewise defined polynomials of degrees one or less (Prenter, 1975). Formula (A.3.1.1) produces estimates which are easily shown by standard multivariate Taylor series analysis to be $O(\Delta x^2_{i-1} + \Delta y^2_{j-1})$ accurate, which is in line with the low order accuracy of the approximate discrete

transport and fate equation. The other three subregions yield similar formulas with the particle tracking concept being carried over from one region to the next. The Fortran 77 encoded program LT3VSI contains the formulas for all four subregions induced about every interior node.

Unfortunately the bilinear Lagrange interpolation procedure, defined as alternative 1, carries with it a great deal of numerical diffusion (Baptista et al., 1984), which can be reduced only be using very small Δx, Δy combinations. But, close spacing of the nodes results in a very large number of nodal points which means that large systems of equations must be solved. Thus the procedure has the disadvantage of being slow and limited by computer storage and speed. The problem of numerical diffusion is magnified in regions of high seepage velocities. Reasons for the large numerical diffusion associated with this interpolation procedure are discussed in detail by Baptista (1987) for the one-dimensional case.

Since the flow field is assumed to be constant, the coordinates of the point P^*_{ijn} are defined by the equations

$$x_i^* = x_i - V_x^* \Delta t \qquad \text{(A.3.1.2)}$$

and

$$y_j^* = y_j - V_y^* \Delta t \quad . \qquad \text{(A.3.1.3)}$$

Substitution of these quantities into the bilinear form (A.3.1.1) obtains

$$\tilde{C}^*(P^*_{ijn}) = C_{rx}\, C_{ry}\, \tilde{C}^*_{i-1,j-1,n} + (1 - C_{rx})C_{ry}\, \tilde{C}^*_{i,j-1,n}$$

$$+ C_{rx}(1 - C_{ry})\, \tilde{C}^*_{i-1,j,n} + (1 - C_{rx})(1 - C_{ry})\, \tilde{C}^*_{i,j,n} \; . \qquad \text{(A.3.1.4)}$$

At the arbitrary point (x_ℓ, y_m) the approximate transport and fate equation (5.3.4) operating under the special hypothesis becomes

$$\tilde{C}^*_{\ell,n,n+1} = C_{rx}\, C_{ry}\, \tilde{C}^*_{\ell-1,m-1,n} + (1 - C_{rx})C_{ry}\, \tilde{C}^*_{\ell,n-1,n}$$

$$+ C_{rx}(1 - C_{ry})\, \tilde{C}^*_{\ell y,m,n} + (1 - C_{rx})(1 - C_{ry})\, \tilde{C}^*_{\ell,m,n}$$

$$+ \frac{D^*_{xy}\,\Delta t}{2\Delta x\Delta y(1 + R^*)}\, \tilde{C}^*_{\ell-1,m-1,n} + \frac{D^*_{xx}\,\Delta t}{\Delta x^2(1 + R^*)}\, \tilde{C}^*_{\ell-1,m,n}$$

$$- \frac{D^*_{xy}\,\Delta t}{2\Delta x\Delta y(1 + R^*)}\, \tilde{C}^*_{\ell-1,m+1,n} + \frac{D^*_{yy}\,\Delta t}{\Delta y^2(1 + R^*)}\, \tilde{C}^*_{\ell,m-1,n}$$

$$- 2\left[\left(\frac{D^*_{xx}\,\Delta t}{\Delta x^2} + \frac{D^*_{yy}\,\Delta t}{\Delta y^2}\right)/(1 + R^*)\right] \tilde{C}^*_{\ell,m,n}$$

$$+ \frac{D^*_{yy}\,\Delta t}{\Delta y^2(1 + R^*)}\, \tilde{C}^*_{\ell,m+1,n} - \frac{D^*_{xy}\,\Delta t}{2\Delta x\Delta y(1 + R^*)}\, \tilde{C}^*_{\ell+1,m-1,n}$$

$$+ \frac{D^*_{xx}\,\Delta t}{\Delta x^2(1 + R^*)}\, \tilde{C}^*_{\ell+1,m,n} + \frac{D^*_{xy}\,\Delta t}{2\Delta x\Delta y(1 + R^*)}\, \tilde{C}^*_{\ell+1,m+1,n} \quad . \qquad \text{(A.3.1.5)}$$

A standard multivariate Taylor series analysis applied to equation (A.3.1.5) shows the total diffusion coefficient in each coordinate to be of the form

$$D^*_{xx_{tot}} = D^*_{xx} + \frac{V^*_x \Delta x}{2} - \frac{V^{*2}_x \Delta t}{2} \qquad \text{(A.3.1.6)}$$

and

$$D^*_{yy_{tot}} = D^*_{yy} + \frac{V^*_y \Delta y}{2} - \frac{V^{*2}_y \Delta t}{2} \quad . \qquad \text{(A.3.1.7)}$$

The cross term D^*_{xy} is not altered.

The ζ-ηth Fourier component can be written as

$$\tilde{C}^*_{\ell,m,n}(\zeta,\eta) = A_{\ell,m}\,\theta^n\, e^{i(\zeta x_\ell+\eta y_m)} \quad , \tag{A.3.1.8}$$

where $A_{\ell,m}$ is a nonzero amplitude parameter.

Substitution of definition (A.3.1.8) into equation (A.3.1.5) and subsequent simplification yields

$$\begin{aligned}
\theta = {} & C_{rx}\,C_{ry}\,e^{-i(\zeta\Delta x+\eta\Delta y)} + (1 - C_{rx})C_{ry}\,e^{-i\eta\Delta y} \\
& + C_{rx}(1 - C_{ry})\,e^{-i\zeta\Delta x} + (1 - C_{rx})(1 - C_{ry}) \\
& + \frac{D^*_{xy}\,\Delta t}{2\Delta x\Delta y(1 + R^*)}\,e^{-i(\zeta\Delta x+\eta\Delta y)} + \frac{D^*_{xx}\,\Delta t}{\Delta x^2(1 + R^*)}\,e^{-i\zeta\Delta x} \\
& - \frac{D^*_{xy}\,\Delta t}{2\Delta x\Delta y(1 + R^*)}\,e^{-i(\zeta\Delta x-\eta\Delta y)} + \frac{D^*_{yy}\,\Delta t}{\Delta x^2(1 + R^*)}\,e^{-i\eta\Delta y} \\
& - 2\left[\left(\frac{D^*_{xx}\,\Delta t}{\Delta x^2} + \frac{D^*_{yy}\,\Delta t}{\Delta y^2}\right)/(1 + R^*)\right] \\
& + \frac{D^*_{yy}\,\Delta t}{\Delta y^2(1 + R^*)}\,e^{i\eta\Delta y} - \frac{D^*_{xy}\,\Delta t}{2\Delta x\Delta y(1 + R^*)}\,e^{i(\zeta\Delta x-\eta\Delta y)} \\
& + \frac{D^*_{xx}\,\Delta t}{\Delta x^2(1 + R^*)}\,e^{i\zeta\Delta x} + \frac{D^*_{xy}\,\Delta t}{2\Delta x\Delta y(1 + R^*)}\,e^{i(\zeta\Delta x+\eta\Delta y)} \quad .
\end{aligned} \tag{A.3.1.9}$$

Simplifying this representation by using the classical Euler formulas relating complex exponential functions and the circular functions or trigonometric functions obtains the complex number

$$\theta = f_1(\zeta,\eta) - i\, f_2(\zeta,\eta) \tag{A.3.1.10}$$

where

$$f_1(\zeta,\eta) = (1 - C_{rx})(1 - C_{ry}) + C_{rx})(1 - C_{ry}) \cos(\zeta\Delta x)$$

$$+ (1 - C_{rx})(C_{ry}) \cos(\eta\Delta y) + C_{rx})(C_{ry}) \cos(\zeta\Delta x + \eta\Delta y)$$

$$-\frac{2D^*_{xx}\ \Delta t}{\Delta x^2(1+R^*)} [1 - \cos(\zeta\Delta x)] - \frac{2D^*_{xy}\ \Delta t}{\Delta x\Delta y(1+R^*)} \sin(\zeta\Delta x) \sin(\eta\Delta y)$$

$$-\frac{2D^*_{yy}\ \Delta t}{\Delta y^2(1+R^*)} [1 - \cos(\zeta\Delta y)] \qquad \text{(A.3.1.11)}$$

and

$$f_2(\zeta,\eta) = C_{rx}(1 - C_{ry}) \sin(\zeta\Delta x) + (1 - C_{rx})C_{ry} \sin(\eta\Delta y)$$

$$+ C_{rx}\ C_{ry} \sin(\zeta\Delta x + \eta\Delta y) \quad . \qquad \text{(A.3.1.12)}$$

In polar form we may write

$$\theta = R_A(\zeta,\eta)\ e^{-i\Phi_A(\zeta,\eta)} \qquad \text{(A.3.1.13)}$$

where

$$R_A = (f_1^2 + f_2^2)^{1/2} \qquad \text{(A.3.1.14)}$$

and

$$\Phi_A = \mathrm{Tan}^{-1}\left(\frac{f_2}{f_1}\right) = \Phi_{Ax}(\zeta,\eta) + \Phi_{Ay}(\zeta,\eta) \quad . \qquad \text{(A.3.1.15)}$$

Clearly, from complex number theory

$$\theta^n = R_A^n(\zeta,\eta)\ e^{-in\Phi_A(\zeta,\eta)} \quad . \qquad \text{(A.3.1.16)}$$

Back substitution of θ^n into (A.3.1.8) obtains the $\zeta\eta$th Fourier component

$$\bar{C}^*_{\ell,m,n}(\zeta,\eta) = A_{\ell,m}\, R_A^n(\zeta,\eta)\, e^{i(\zeta x_\ell + \eta y_m - n\Phi_A(\zeta,\eta))} \quad . \qquad (A.3.1.17)$$

The approximate solution then assumes the form

$$\bar{C}^*(x_\ell, y_m, t_n) = \frac{1}{4\pi^2} \int_{-\infty}^{+\infty} \int_{-\infty}^{+\infty} \hat{C}(\zeta,\eta,0^+)\, R_A^n(\zeta,\eta) \bullet$$

$$e^{i\zeta(x_\ell - t_n \frac{\Phi_{Ax}}{\zeta\Delta t})}\, e^{i\eta(y_m - t_n \frac{\Phi_{Ay}}{\eta\Delta t})}\, d\zeta\, d\eta \quad . \qquad (A.3.1.18)$$

Comparing the structure of R_A, defined by equation (A.3.1.14), with the more simple structure of R_E, defined by equation (A.2.9) shows that even with the single 4-point bilinear interpolation scheme, the amplitude for each time step function is extremely complicated. The phase angle for each time step function is also a complicated function of ζ and η, not simply a linear function of ζ and η such as Φ_E is. Careful inspection of equations (A.3.1.11) and (A.3.1.13) reveals that whenever $\zeta\Delta x$ and $\eta\Delta x$ are multiples of 2π radians, f_1 and f_2 repeat themselves, regardless of the Courant numbers or the other parameters which appear in these equations. This periodicity stands in contrast to the monotonic function of R_E as defined by equation (A.2.9). At the points where $\zeta\Delta x$ and $\eta\Delta x$ are multiples of 2π radians, $R_A \equiv 1$ and $\Phi_A \equiv 0$ so that the Fourier components suffer no attenuation and do not propagate in space, as time evolves. Because both R_A and Φ_A are periodic functions of ζ and η only the basic rectangular region in IR^2 which consist of the set of all (ζ,η) such that $0 \le \zeta \le 2\pi/\Delta x$ and $0 \le \eta \le 2\pi/\Delta y$ needs to be considered. Figure A.3 shows the placement of the basic regions in the Eucledian plane, IR^2. For evaluation of R_A and Φ_A all other values of (ζ,η) are aliases of this basic region (Bloomfield, 1976).

Since both R_A and Φ_A are periodic functions of ζ and η, the long time character of the approximate distribution $C^*(x,y,t)$ depends upon the character or shape of the double Fourier transform of the initial distribution $C^*(\zeta,\eta,0^+)$, for initial value problems or for the double Fourier transform of the source function, if any sources exist. Table A.1 shows the values of the functions R_E, ΦE, R_A, and Φ_A per time step function $R_A(\zeta,\eta)$ over the basic region of definition for the following geometric and transport parameter values: $\Delta x = \Delta y = 1.0$ meter, $V_x = 0.0$ m/day, $V_y = 0.55$ m/day, $D_{xx} = 0.002$ m^2/day, $D_{xy} = 0.0$ m/day, $D_{yy} = 0.002$ m^2/day, $t = 0.001$ day. Table A.1 also shows the results of evaluating the phase angle per time step function $\Phi_A(\zeta,\eta)$ over the basic region of definition. For comparison purposes the exact amplitude per time step R_E and the exact phase angle Φ_E are included in Table A.1. Using the value of $\Delta t = 0.001$ day requires 20,000 time steps for a simulation 20 days long. Thus, n = 20,000 at 20 days. Table A.2 shows the values of the amplitudes and phase angles at time t = 20 days for the basic region. Recall that (Figure A.3) the approximate amplitudes and phase angles outside the basic region are found from aliasing. The exact amplitudes and phase angles <u>do not</u> follow this simple aliasing procedure.

Careful study of Table A.2 shows that by the time 20 days have elapsed the approximate amplitude factors have decayed to negligible value except in tight clusters around integer multiples of 2π in each coordinate. That is, only in the neighborhood of those $(\zeta\Delta x,\eta\Delta y) = (p\pi,q\pi)$, p or q or both even integers, is $R_A{}^n$ still significant when n = 20,000 time steps. However, these are precisely the Fourier components which <u>do not</u> propagate at all. Negative signs indicate waves

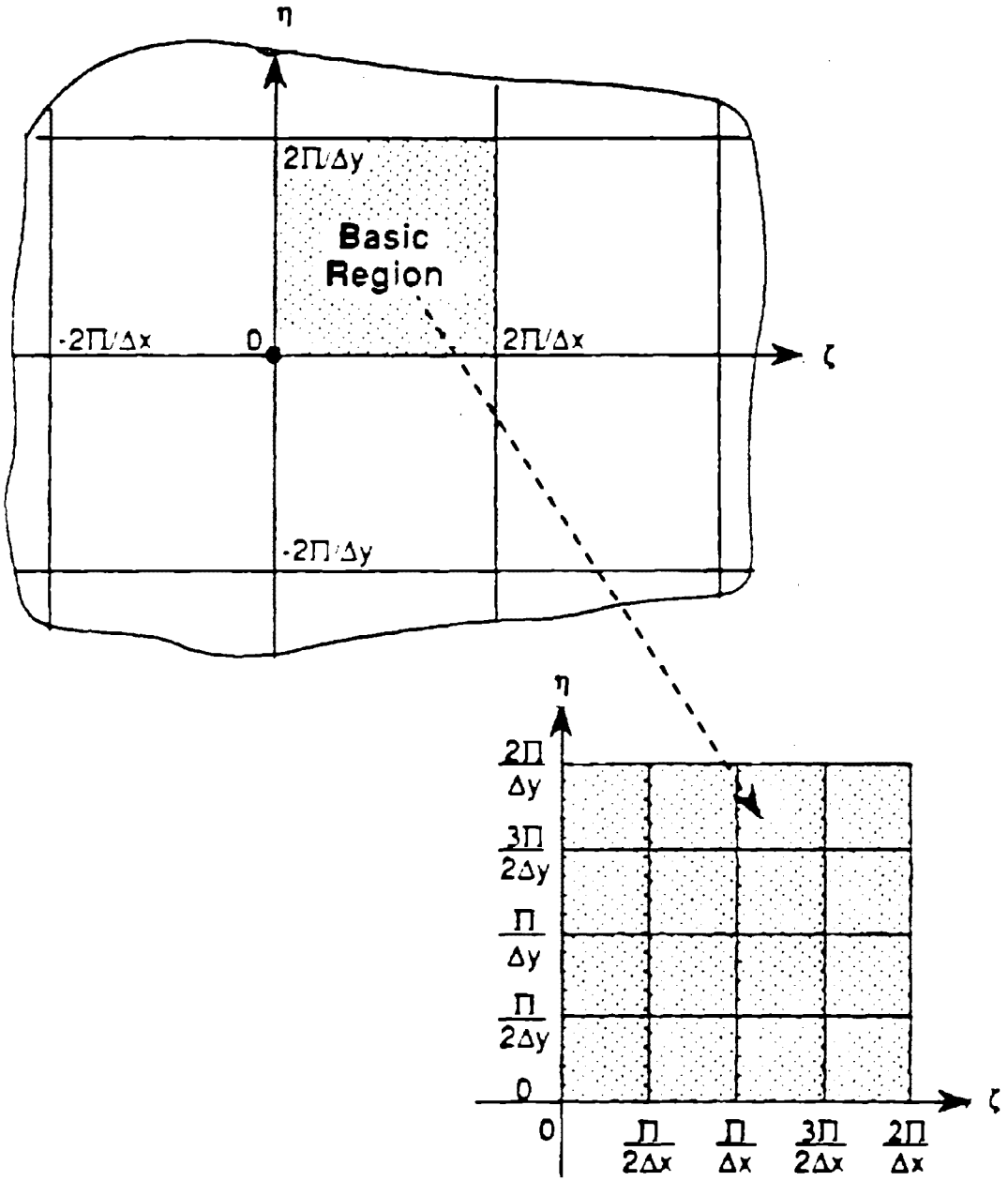

Figure A.3. Placement of the basic region of definition in IR^2.

Table A.1. Evaluation of R_E, ΦE, R_A, and Φ_A in the illustrative data corresponding to a simple constant longitudinal Darcian flow field and a uniform mesh spacing. The units for R_E and R_A are (1/time step) and for Φ_E and Φ_A they are (rad/time step).

$\zeta\Delta x$	$\eta\Delta y$	R_E	Φ_E	R_A	Φ_A
		(time step)$^{-1}$	(rad/time step)$^{-1}$	(time step)$^{-1}$	(rad/time step)$^{-1}$
0	0	1.000000	0.000000	1.000000	0.000000
0	$\pi/2$	0.999995	8.63938 E-04	0.999448	5.50304 E-04
0	π	0.999980	1.72788 E-03	0.998896	0.000000
0	$3\pi/2$	0.999956	2.59181 E-03	0.999448	-5.50304 E-04
0	2π	0.999921	3.45575 E-03	1.000000	0.000000
$\pi/2$	0	0.999995	0.00000	0.999996	0.000000
$\pi/2$	$\pi/2$	0.999990	8.63938 E-04	0.998888	5.50307 E-04
$\pi/2$	π	0.999975	1.72788 E-03	0.998888	0.000000
$\pi/2$	$3\pi/2$	0.999951	2.59181 E-03	0.999442	-5.50307 E-04
$\pi/2$	2π	0.999916	3.45575 E-03	0.999996	0.000000
π	0	0.999980	0.00000	0.999992	0.000000
π	$\pi/2$	0.999975	8.63938 E-04	0.999438	5.50309 E-04
π	π	0.999961	1.72788 E-03	0.998884	0.000000
π	$3\pi/2$	0.99936	2.59181 E-03	0.999438	-5.50309 E-04
π	2π	0.999901	3.45575 E-03	0.999992	0.000000
$3\pi/2$	0	0.999956	0.00000	0.999996	0.000000
$3\pi/2$	$\pi/2$	0.999951	8.63938 E-04	0.999442	5.50307 E-04
$3\pi/2$	π	0.999936	1.72788 E-03	0.998888	0.000000
$3\pi/2$	$3\pi/2$	0.999911	2.59181 E-03	0.999442	-5.50307 E-04
$3\pi/2$	2π	0.999877	3.45575 E-03	0.999996	0.000000
2π	0	0.999921	0.00000	1.000000	0.000000
2π	$\pi/2$	0.999916	9.63938 E-04	0.999446	5.50305 E-04
2π	π	0.999901	1.72788 E-03	0.998892	0.000000
2π	$3\pi/2$	0.999877	2.59181 E-03	0.999446	-5.05305 E-04
2π	2π	0.999842	3.45575 E-03	1.000000	0.000000

Table A.2. Evaluation of R_E^n, $n\Phi E$, R_A^n, and $n\Phi_A$ for the data given in Table A.1.

$\zeta\Delta x$	$\eta\Delta y$	R_E^n	$n\Phi_E$	R_A^n	$n\Phi_A$
0	0	1.000000	0.00000	1.000000	0.000000
0	$\pi/2$	0.904837	17.27876	0.000015	11.00610
0	π	0.670317	34.5576	0.000000	0.000000
0	$3\pi/2$	0.414775	51.8362	0.000015	-11.00610
0	2π	0.205962	69.1150	1.000000	0.000000
$\pi/2$	0	0.904837	0.00000	0.923116	0.000000
$\pi/2$	$\pi/2$	0.818729	17.27876	0.000014	11.00614
$\pi/2$	π	0.606526	34.5576	0.000000	0.000000
$\pi/2$	$3\pi/2$	0.375302	51.8362	0.000014	-11.00614
$\pi/2$	2π	0.186360	69.1150	0.923116	0.000000
π	0	0.670317	0.00000	0.852143	0.000000
π	$\pi/2$	0.606526	17.27876	0.000018	11.00618
π	π	0.458399	34.5576	0.000000	0.000000
π	$3\pi/2$	0.278025	51.8362	0.000013	-11.00618
π	2π	0.138055	69.1150	0.852143	0.000000
$3\pi/2$	0	0.414774	0.00000	0.923116	0.000000
$3\pi/2$	$\pi/2$	0.375302	17.27876	0.000014	11.00614
$3\pi/2$	π	0.278025	34.5576	0.000000	0.000000
$3\pi/2$	$3\pi/2$	0.168624	51.8362	0.000014	-11.00614
$3\pi/2$	2π	0.085422	69.1150	0.923116	0.000000
2π	0	0.205962	0.00000	1.000000	0.000000
2π	$\pi/2$	0.186360	17.27876	0.000015	11.00610
2π	π	0.138055	34.5576	0.000000	0.000000
2π	$3\pi/2$	0.085422	51.8362	0.000015	-11.00610
2π	2π	0.042415	69.1150	1.000000	0.000000

propagating in the leftward direction. It appears that only those Fourier components whose frequencies $\zeta\Delta x$ and $\eta\Delta y$ fall in $[0,\pi/2]$ propagate reasonably well. The disparity between the phase angles, $n\Phi_E$ and $n\Phi_A$ for in between values of ζ and η is obvious. Clearly as time evolves, shrinking sized island of area centered about $(p\pi,q\pi)$ being to appear as the dominant areas which contribute to the actual approximate distribution $C^*(x_p,y_q,t_n)$. The extent of the wiggles depends largely then upon the magnitude of the tail regions (mid to high frequency components) of the double Fourier transform of $C^*(x,y,0^+)$; namely, $C^*(\zeta,\eta,0^+)$. If distribution $C^*(,,0+)$ has considerable high frequency information in it, e.g. the double Fourier transform of a vertically sided rectangular distribution of constant amplitude, Amp, and of dimensions δx_s by δy_s referenced to corner point (x_s,y_s), i.e.

$$F(\zeta,\eta) = 4\text{Amp}\ e^{-i\zeta(x_s+\frac{\delta x_s}{2})}\ e^{-i\eta(y_s+\frac{\delta y_s}{2})} \bullet \frac{\sin(\zeta\frac{\delta x_s}{2})}{\zeta} \bullet \frac{\sin(\eta\frac{\delta y_s}{2})}{\eta}, \quad (A.3.1.19)$$

then a large number of terms including those well outside the basic region must be retained to faithfully represent $C^*(x_\ell,y_m,t_n)$. If distribution $C^*(\zeta,\eta,0^+)$ consists of mainly low frequency components, e.g. the double Fourier transform of a two-dimensional Gausshill centered at (x_s,y_s) and of amplitude, Amp, with shaping done by the two "variance" parameters σ_x^2 and σ_y^2, i.e.

$$F(\zeta,\eta) = \text{Amp}\ e^{-i(\zeta x_s+\eta y_s)}\ e^{-(\frac{\sigma_x^2\zeta^2}{2}+\frac{\sigma_y^2\eta^2}{2})}, \quad (A.3.1.20)$$

then only a few low frequency terms may be necessary to retain a faithful representation $C^*(x_\ell,y_m,t_n)$, especially if σ_x^2 and σ_y^2 are large variances.

A.3.2 Alternative 2: Biquartic Lagrange Polynomials

Baptista (1987) gives an extensive discussion of the linear, quadratic, cubic, quartic, and cubic-Hermite polynomial based methods of interpolation or estimation of $C^*(P_{i,n})$ for the one-dimensional transport case, using tables and graphs showing the amplitudes and phases of the Fourier components. The underlying solution theory for linear parabolic transport and fate problems readily allows the extension of these one-dimensional concepts to two and three dimensional linear transport and fate problems. The one-dimensional quartic (4th degree) Lagrange interpolation structure presented by Baptista (1987) is extended to a biquartic (4th degree in each variable) Lagrange interpolation structure. Note that a 4th degree polynomial is needed in order to be able to uniquely Lagrange interpolate five distinct points of a univariate function defined on the interval $[x_{i-2}, x_{i+2}]$, for $i = 2,3,\ldots N_x-2$. Therefore, for a two dimensional domain of definition, 25 distinct points are required for a biquartic interpolation formula. The Lagrange bicanonical basis form is the easiest structure to work with in this case. Define the biquartic Lagrange approximation to be

$$\tilde{C}^* (P^*_{ijn}) = \sum_{q=1}^{5} \sum_{p=1}^{5} \ell_{p,q}(x^*_{i(n)}, y^*_{j(n)}) \bar{C}^*_{i-3+p,j-3+q,n} \qquad (A.3.2.1)$$

where

$$\ell_{pq}(x^*_{i(n)}, y^*_{j(n)}) = \frac{P_{px}(x^*_{i(n)})}{P_{px}(x_{i-3+q})} \bullet \frac{P_{qy}(y^*_{j(n)})}{P_{qy}(y_{j-3+q})} \qquad (A.3.2.2)$$

for each i,j combination in the superinterior of the lattice of nodal points, where superinterior refers to those interior points which lie beyond at least one line of points inside the boundary line of points.

Figure A.4 shows the acceptable region when points are close to the domain boundaries. Concentrations $C^*(P^*_{ijn})$ at points outside of the region of acceptability are estimated using the bilinear Lagrange procedure previously discussed.

The polynomials $P_{px}*$ and $P_{qy}*$ of equation (A.3.2.2) are defined as follows for centering on nodal point (x_i, y_j):

$$P_{1x} = (x - x_{i-1})(x - x_i)(x - x_{i+1})(x - x_{i+2}), \tag{A.3.2.3}$$

$$P_{2x} = (x - x_{i-2})(x - x_i)(x - x_{i+1})x - x_{i+2}), \tag{A.3.2.4}$$

$$P_{3x} = (x - x_{i-2})(x - x_{i-1})(x - x_{i+1})(x - x_{i+2}), \tag{A.3.2.5}$$

$$P_{4x} = (x - x_{i-2})(x - x_{i-1})(x - x_i)(x - x_{i+2}), \tag{A.3.2.6}$$

$$P_{5x} = (x - x_{i-2})(x - x_{i-1})(x - x_i)(x - x_{i+1}), \tag{A.3.2.7}$$

and

$$P_{1y} = (y - y_{j-1})(y - y_j)(y - y_{j+1})(y - y_{j+2}), \tag{A.3.2.8}$$

$$P_{2y} = (y - y_{j-2})(y - y_j)(y - y_{j+1})(y - y_{j+2}), \tag{A.3.2.9}$$

$$P_{3y} = (y - y_{j-2})(y - y_{j-1})(y - y_{j+1})(y - y_{j+2}), \tag{A.3.2.10}$$

$$P_{4y} = (y - y_{j-2})(y - y_{j-1})(y - y_j)(y - y_{j+2}), \tag{A.3.2.11}$$

$$P_{5y} = (y - y_{j-2})(y - y_{j-1})(y - y_j)(y - y_{j+1}). \tag{A.3.2.12}$$

It is a laborious but straightforward task to show that the bilinear form of interpolation formula (A.3.1.1) has no numerical diffusion in the case of a lossless transport equation. The absence of numerical diffusion with the biquartic interpolation formula would be

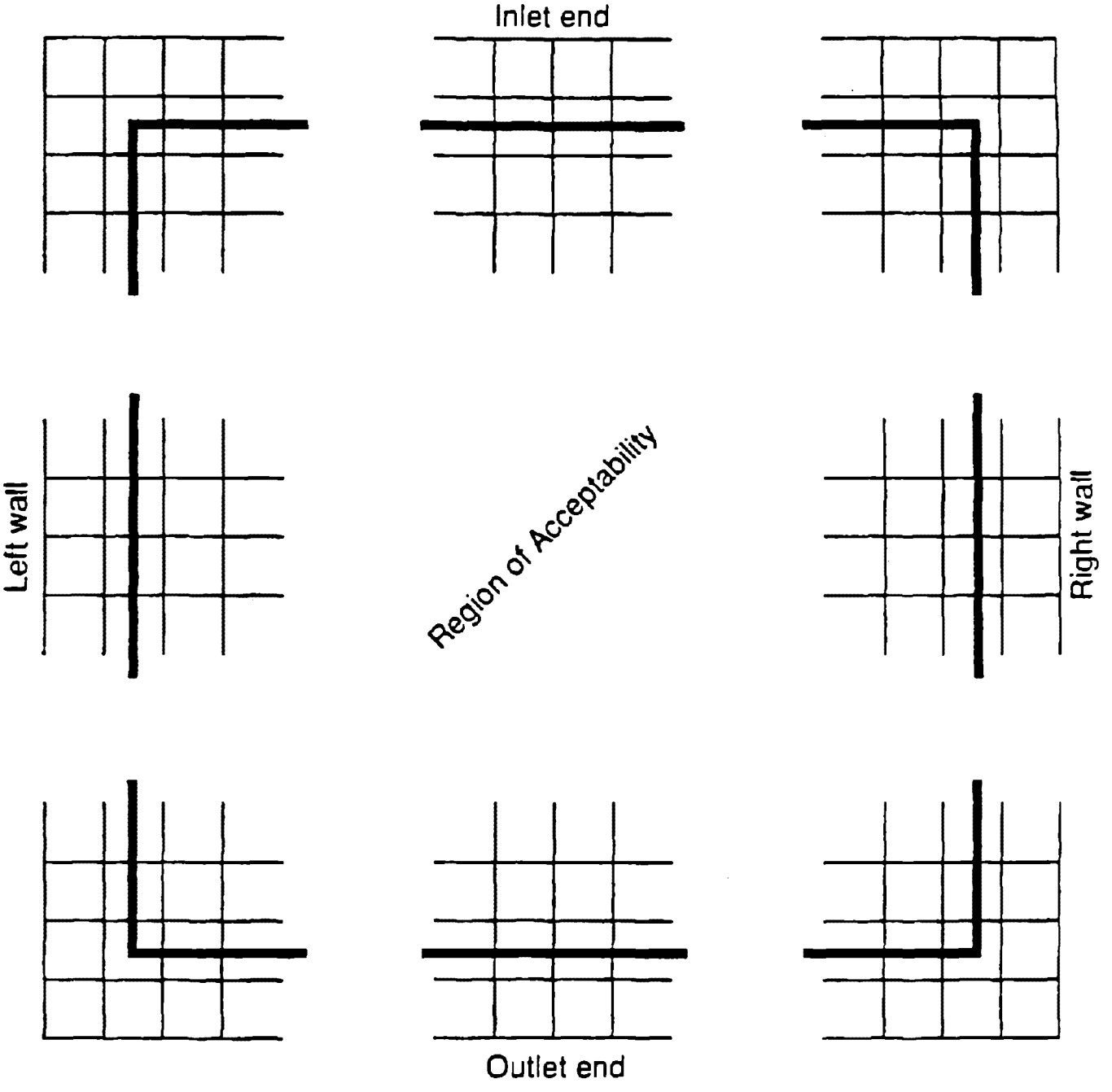

Figure A.4. Two-dimensional lattice of nodal points superimposed on IR^2 showing the region of acceptability for the 25 point interpolation alternative.

expected since the one space dimensional version was shown to have no numerical diffusion (Baptista, 1987). The price paid for the elimination of numerical diffusion is the occurrence of small "oscillations" or "wiggles" near the regions of rapid transition or change in concentration. This numerical problem was expected to occur, based on the knowledge about the one space dimensional case. The oscillations or wiggles near a leading front and a trailing edge which occur in the multidimensional transport case, where multidimensional Lagrange interpolating polynomials of degree 2 or higher in each space variable are used, are hypothesized to be caused by the different amplitude factors and the different propagation velocities of the multidimensional Fourier harmonic components in the exact solution of the approximating finite difference (discrete) equations when compared to the exact solution of the continuous parabolic transport and fate equation. As was done in alternative 1, the bilinear Lagrange interpolating polynomials, using the above outlined specialized hypothesis on the flow domain, it is possible to double Fourier analyze the approximate distribution $C^*(x,y,t)$ at domain point (x_ℓ, y_m) at time t_n. The approximation for $C^*(P_{ijn})$, analogous to equation (A.3.14), is now a linear combination of 25 coefficient functions of C_{rx} and C_{ry}, each multiplying one of the 25 concentrations in the advection molecule centered at nodal point (x_ℓ, y_m). Then the form (A.3.1.6) can be substituted into the analogous expression to (A.3.1.5), and θ obtained for the biquartic procedure. Finally, θ can be expressed in polar form with the final result being the biquartic approximate distribution analogue of equation (A.3.1.16). The only changes will be in functions $f_1(\zeta,\eta)$, definition (A.3.1.9), and $f_2(\zeta,\eta)$, definition (A.3.1.10).

These functions will be much more complicated functions of C_{rx}, C_{ry}, $\zeta\Delta x$, and $\eta\Delta y$ than the bilinear derived forms. We choose not to list these extremely awkward functions here, and simply rely on the results of the one-dimensional analysis done by Baptista (1987). However, further work is planned since in the multidimensional case this is still a largely unexplored area of research.

Experience gained with the biquartic method shows that to use the method, the investigator must be very careful in representing his initial data and his source data. The use of steep sided distributions or source regions produced wiggles of about 5% the maximum concentration early on in the above mentioned special hypothesis two-dimensional flow problem. Using a smooth sided two-dimensional Gausshill initial distribution, wiggles, whose amplitude grew asymptotically in time to about 0.2% of the peak or maximum value, were produced. This is a much more satisfactory situation.

TECHNICAL REPORT DATA
(Please read Instructions on the reverse before complete)

1. REPORT NO. EPA/600/2-91/014	2.	3.
4. TITLE AND SUBTITLE DENITRIFICATION IN NONHOMOGENEOUS LABORATORY SCALE AQUIFERS: 4. HYDRAULICS, NITROGEN CHEMISTRY, AND MICROBIOLOGY IN A SINGLE LAYER		5. REPORT DATE April 1991
		6. PERFORMING ORGANIZATION CODE
7. AUTHOR(S) F.T. Lindstrom, L. Boersma, D. Myrold, and M. Barlaz		8. PERFORMING ORGANIZATION REPORT NO.
9. PERFORMING ORGANIZATION NAME AND ADDRESS Department of Soil Science, Oregon State University, Corvallis, OR 97331		10. PROGRAM ELEMENT NO. CBWD1A
		11. CONTRACT/GRANT NO. CR-814502
12. SPONSORING AGENCY NAME AND ADDRESS U.S. Environmental Protection Agency, Robert S. Kerr Environmental Research Laboratory, P.O. Box 1198, Ada, OK 74820		13. TYPE OF REPORT AND PERIOD COVERED Final Report
		14. SPONSORING AGENCY CODE

15. SUPPLEMENTARY NOTES

Project Officer: Thomas E. Short FTS: 743-2292

16. ABSTRACT

A two-dimensional mathematical model for simulating the transport and fate of organic chemicals in a laboratory scale, single layer aquifer is presented. The aquifer can be nonhomogeneous and anisotropic with respect to its fluid flow properties. The physical model has open inlet and outlet ends and is bounded by impermeable walls on all sides. Fully penetrating injection and/or extraction wells can be placed anywhere in the flow field. The inlet and outlet boundaries have user prescribed hydraulic pressure fields. The steady state hydraulic pressure field is obtained first by using the two-dimensional Darcy flow law and the continuity equation. The chemical transport and fate equation is then solved in terms of user stipulated initial and boundary conditions. The model accounts for the major physical processes of storage, dispersion, and advection, and also can account for linear equilibrium sorption, first-order loss processes, microbial denitrification, irreversible sorption and/or dissolution into the organic phase, metabolism in the sorbed state, and first order loss in the sorbed state. The chemical may be released internally via distributed leaks, sources that do not perturb the flow field, or fully penetrating injection wells. Chemical compounds may also enter at the inlet boundary. Chemical mass balance type inlet and outlet boundary conditions are used.

17. KEY WORDS AND DOCUMENT ANALYSIS

a. DESCRIPTORS	b. IDENTIFIERS/OPEN ENDED TERMS	c. COSATI Field/Group

18. DISTRIBUTION STATEMENT RELEASE TO PUBLIC	19. SECURITY CLASS (This Report) UNCLASSIFIED	21. NO. OF PAGES 91
	20. SECURITY CLASS (This page) UNCLASSIFIED	22. PRICE

EPA Form 2220-1 (Rev. 4-77) PREVIOUS EDITION IS OBSOLETE